Phthalimido-ferrocidiphenol cyclodextrin complexes: Characterization and anticancer activity

Feten Najlaoui, Pascal Pigeon, Zaineb Abdelkafi, Sebastien Leclerc, Pierrick Durand, Mohamed El Ayeb, Naziha Marrakchi, Ali Rhouma, Gérard Jaouen, Stéphane Gibaud

Phthalimido-ferrocidiphenol cyclodextrin complexes: characterization and anticancer activity

Feten Najlaoui[a,f,g], Pascal Pigeon[b,c], Zaineb Abdelkafi[a], Sebastien Leclerc[d], Pierrick Durand[e], Mohamed El Ayeb[a], Naziha Marrakchi[a], Ali Rhouma[f], Gérard Jaouen[b,c], Stéphane Gibaud[g*]

[a] Institut Pasteur de Tunis, Laboratoire des Venins et Biomolécules Thérapeutiques LR11IPT08, 13, Place Pasteur, 1002 Tunis, Tunisia

[b] Chimie ParisTech, 11 rue Pierre et Marie Curie, Paris F-75231 Paris Cedex 05, France

[c] Sorbonne Universités, UPMC Université Paris 6, Institut Parisien de Chimie Moléculaire (IPCM), UMR 8232, 4 Place Jussieu, 75252 Paris Cedex 05, France

[d] Université de Lorraine, LEMTA, UMR 7563, Faculté des Sciences et Technologies, Boulevard des Aiguillettes, Vandœuvre-lès-Nancy, F-54500, France

[e] Université de Lorraine/CNRS, CRM2, UMR 7036, Faculté des Sciences et Technologies, Boulevard des Aiguillettes, Vandœuvre-lès-Nancy, F-54500, France

[f] Olive Tree Institute, Research Unit of Plant Protection and Environment, Mahrajene City BP 208, 1082 Tunis, Tunisia

[g] Université de Lorraine, EA 3452 / CITHEFOR, 5 rue Albert Lebrun (Faculté de Pharmacie), F-54000 Nancy, France

*Corresponding author:
Université de Lorraine, EA 3452 / CITHEFOR, 5 rue Albert Lebrun (Faculté de Pharmacie), F-54000 Nancy, France. Tel.: +33 3 83 68 23 10; fax: +33 3 83 68 23 01.
E-mail address: stephane.gibaud@univ-lorraine.fr.

Abstract

Several ferrocenyl analogues of tamoxifen have already showed strong antiproliferative activity in experimental glioma models. Nevertheless, these compounds are very poorly soluble in water and an adapted formulation is needed.

In this work, we have tailored and optimized methylated cyclodextrin soluble complexes of phthalimido-ferrocidiphenol for the first time. The complexes were characterized, and the optimized formulation was tested for *in vitro* efficacy and cell proliferation assays on U87, human glioblastoma cancer cells.

Molecular modeling can provide accurate information about the inclusion process. The inclusion of all the moieties at the same time (i.e., ferrocene, phthalimidylpropyl, 2 phenols) is not possible due to the steric hindrance of the 1:4 system. The 1:3 systems are possible but do not seem very relevant. However, various 1:2 and 1:1 complexes are mostly present in aqueous solutions.

Some experiments have confirmed our hypothesis. First, interactions between the phenol, phthalimidylpropyl and ferrocenyl groups have been observed in our NMR experiments. Second, the inclusion of phthalimidylpropyl was detected by UV-vis spectrophotometry with an apparent 1:1 interaction, which was observed through the Benesi-Hildebrand method.

The complex is readily soluble in water and keeps its pharmacological activity against U87 tumor cells (IC_{50} = 0.028 ± 0.007 µM *vs.* 0.018 ± 0.003 µM for PhtFerr).

Keywords: ferrocene; organometallic; anticancer drug; glioma; cyclodextrin

1. Introduction

Ferrocene has gained tremendous attention in the scientific and technical community because of its captivating chemistry (Rosenblum, 1965; Togni and Hayashi, 1994). Different strategies have been adopted to develop ferrocene derivatives and to explore their wide-ranging scientific applications.

Ferrocenyl compounds have gained much popularity in biological applications because of their stability in aqueous and aerobic media, access to a great variety of derivatives, and their promising electrochemical properties: the toxic agent in the cell can eventually transform into an oxidized and reactive molecule. Thus, we have proven that molecules bearing the [ferrocenyl-ene-phenol] motif can be oxidized into a quinone methide (Buriez et al., 2008; Messina et al., 2012; Wang et al., in press) able to react with a SH moiety, as in some proteins, or on the selenocysteine residue of thioredoxin reductases (Citta et al., 2014). The formation of this molecule is due to the redox properties of ferrocene (Hillard et al., 2010; Swarts et al., 1994). More specifically, recent studies have shown a high activity of ferrocene derivatives *in vitro* and *in vivo* against a variety of fungal and bacterial infections (Biot et al., 2000; Zhang, 2008), e.g., malaria (Biot et al., 1997; Fouda et al., 2007; Itoh et al., 2000), HIV (Kondapi et al., 2006) and cancer (Hillard et al., 2010; Swarts et al., 1994). After these results, the medicinal use of ferrocene became plausible.

Consequently, a variety of ferrocenyl compounds are being synthesized and tested for their anticancer properties. Among all ferrocene derivatives, ferrocifens (Jaouen and Top, 2013) have encouraging effects against breast cancer (Hillard et al., 2010; Nguyen et al., 2007). Recently, the non-steroidal selective estrogen receptor modulator (SERM), tamoxifen, has been commonly prescribed for patients diagnosed with estrogen-receptor-positive (or ER+) breast cancer (Craig Jordan, 1992). The first coupling of ferrocene to the active metabolite of tamoxifen was done by G. Jaouen and his co-workers by replacing a phenyl group of 4-hydroxytamoxifen with ferrocene (Ornelas, 2011). These hydroxyferrocifens were intended to combine the antiestrogenic properties

of tamoxifen while targeting the ferrocenyl moiety to the receptor and thus to DNA for a possible gain in therapeutic benefits (Top et al., 1996; Top et al., 2003).

In addition to the effect of the quinone methide, it was also suggested that DNA damage due to hydroxyl radical production causes the toxicity of the ferrocenium cation (Tamura and Miwa, 1997). To bring ferrocene in close proximity to DNA, the ferrocenyl group can be attached to molecules that bind DNA, which might enhance the probability of DNA damage and cell apoptosis (Ornelas, 2011).

The molecules bearing the [ferrocenyl-ene-phenol] motif, which are needed to form the reactive quinone methides *in vivo*, are called the ferrociphenol series. The hydroxyferrocifen series bearing this motif (and also a dimethylaminoalkyl chain inherited from the tamoxifen) belong to this larger family. The replacement of this chain by a second phenol group led to the ferrocidiphenol family, a sub-series of the ferrociphenol series (Figure 1), without many change in the activity, and with the advantage of having a smaller size and avoiding formation of a Z/E isomers mixture. Thus, a series of ferrociphenols [ferrocifens (Top et al., 2003), ferrocidiphenol (Vessieres et al., 2005), and cyclic ferrocidiphenols (Plazuk et al., 2009)] that was evaluated for their antiproliferative activity against breast cancer displayed low IC_{50} values (between 0.09 and 13 µM) (Hillard et al., 2010). Additionally, several ferrocenyl analogues of tamoxifen have already showed a strong antiproliferative activity on experimental glioma models (Laine et al., 2013; Roger et al., 2012). This property is a matter of interest, as glioblastoma, which is the most common malignant glioma, has only been associated to date with a median survival of 12−15 months. In fact, the European Organization for Research and Treatment of Cancer (EORTC) has published a study on the concomitant use of radiation therapy and adjuvant temozolomide, which slightly improved survival (overall survival: 9.8% after 5 years). This treatment is now adopted as the new standard treatment, but it is still not satisfactory (Stupp et al., 2009). Temozolomide is an oral drug that is rapidly metabolized into methyltriazeno-imidazole-carboxamide (MTIC), a DNA-methylating drug. A DNA repair enzyme, methyl-guanine methyltransferase (MGMT), can remove the methyl group and overcome the modification of cells that lack MGMT, which have been shown to have a higher sensitivity to temozolomide. Intrinsic or

acquired resistance often defines the poor efficacy of chemotherapy in malignant gliomas.

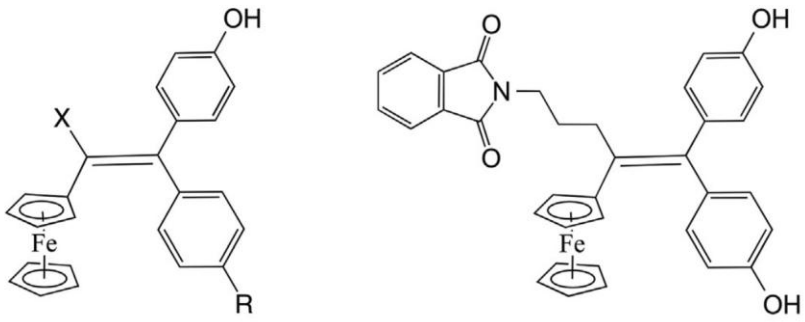

Ferrociphenol series (and sub-series) :
X = Et, R = O-$(CH_2)_n NMe_2$ (ferrocifens series)
R = OH (ferrocidiphenol series)
X = Et, R = OH (ferrocidiphenol molecule)

New derivative of the ferrocidiphenol series : phthalimido-ferrocidiphenol (PhtFerr)

Fig. 1. The chemical structure of phthalimido–ferrocidiphenol: N-{4-ferrocenyl-5,5-bis-(4-hydroxyphenyl)-pent-4-enyl}phthalimide—$C_{35}H_{29}FeNO_4$—Molecular weight: 583.45 g/mol.

Having fixed 3 of the 4 substituents of the central alkene double bond of the ferrocidiphenol molecule (ferrocenyl and 2 phenol moieties), the only degree of freedom was to modify the ethyl group, inherited from the tamoxifen. Fortunately, recent work showed us that modifications sometimes permitted a sensible gain in activity [hydroxylation (Pigeon et al., 2014; Richard et al., 2015; Wang et al., in press) or formation of a ferrocenophane cycle (Plazuk et al., 2009)]. Thus, with this encouraging research on the modification of this ethyl group, a new substituted ferrocidiphenol, a "phthalimido-ferrocidiphenol" (replacement of the ethyl group by a phthalimidylpropyl moiety, PhtFerr, Figure 1), has emerged and become the most effective agent according to *in vitro* antiproliferative assays (on glioma cells U87). Interestingly, PhtFerr was tested on breast cancer cells (0.20 µM on MDA-MB231; 3-fold better than the original ferrocidiphenol molecule) and on human glioblastoma cancer cells (U87), where it was shown to be very active (unpublished results). To date, its mechanism of action is not fully understood, but an oxygenated polar moiety seems to be needed on the alkyl chain replacing the ethyl group (SAR in progress).

This compound (Figure 1) is a highly lipophilic molecule (Log $P_{o/w}$: 5.30) that is very poorly soluble in water (solubility < 0.001 µg/ml). In the last decade, many solutions

have been proposed for the administration of poorly soluble drugs (Bittner and Mountfield, 2002): pH adjustment and co-solvent solutions (Alvarez-Nunez and Yalkowsky, 1999), cyclodextrins (CD) (Buriez et al., 2008; Petrovski et al., 2008), surfactants, mixed micelles (Nguyen et al., 2008; Wei et al., 2010), emulsions (Gibaud and Attivi, 2012), and nanosuspensions (Ben Zirar et al., 2008).

Lipid nanocapsules (LNC) of approximately 50 nm were also used to encapsulate the active ferrocenyl diphenol (ferrocidiphenol or Fc-diOH; Figure 1) tamoxifen derivative in order to allow for a parenteral administration (Allard et al., 2009; Allard et al., 2008). The Fc-diOH (ferrocidiphenol molecule) was encapsulated in high loading because of the large hydrophobic core in the LNC structure. The loaded LNCs were taken up by 9L-glioma cells, and the cytostatic activity of the Fc-diOH was conserved presenting an IC_{50} value of approximately 0.6 µM.

Currently, CD complexes represent one of the most promising and most investigated delivery systems for various lipophilic drugs (Madan et al., 2014; Rodgers et al., 2011), including cancer therapy (Becherirat et al., 2013; Xiong et al., 2014). They are bucket-shaped, cyclic oligosaccharides, comprising 6, 7, or 8 glucopyranose units, linked by α, 1-4-glycosidic bonds (El-Maradny et al., 2008). β-CD has the ability to form stable soluble aggregates with a broad range of lipophilic molecules (Çelik et al., 2011; Soares da Silva et al., 2011). However, the restricted aqueous solubility of β-CD (18.5 mg/ml) presents hurdles in the design and development of soluble complexes of lipophilic drugs (Chatjigakis et al., 1992). Because of their wider cavity size and higher aqueous solubility (>2,000 mg/ml), methylated CDs produce more wettable amorphous complexes with improved water solubility (Banchero et al., 2013). Other derivatives of ß-CD, such as hydroxypropyl-ß-cyclodextrin (HPßCD) and SBEβCD, have similar properties and can be used to improve the solubility of lipophilic drugs.

Therefore, in the present investigation, we have tailored and optimized, for the first time, methylated CD soluble complexes of phthalimido-ferrocidiphenol. The complexes were characterized, and the optimized formulation was tested for *in vitro* efficacy and cell proliferation assays on U87, human glioblastoma cancer cells.

Materials and methods

1.1. Materials

1.1.1. *Chemistry*

The starting materials for the synthesis of PhtFerr were phthalimide, potassium carbonate, *N*,*N*-dimethylformamide, zinc, titanium tetrachloride, tetrahydrofuran (THF) and 4,4'-dihydroxybenzophenone, which were obtained from Sigma-Aldrich (L'Isle d'Abeau Chesnes, 38297 Saint-Quentin, Fallavier, France), TCI EUROPE N.V. (Boerenveldseweg 6, Haven 1063, 2070 Zwijndrecht, Belgique), and Alfa Aesar France (2 allée d'Oslo, 67300 Schiltigheim, France).

All reactions and manipulations were carried out under an argon atmosphere using standard Schlenk techniques. THF was distilled over sodium/benzophenone prior to use. Thin-layer chromatography was performed on silica gel 60 GF_{254}. IR spectra were obtained on a FT/IR-4100 JASCO 180 spectrometer. ^{1}H and ^{13}C NMR spectra were obtained on a Bruker 300 MHz spectrometer. Mass spectrometry was carried out at the Service de Spectrométrie de Masse at ENSCP, Paris. High-resolution mass spectra (HRMS) and RX structures were acquired in the Institut Parisien de Chimie Moléculaire (IPCM – UMR 8232) at the Université Pierre et Marie Curie, Paris.

1.1.2. Other materials

SBEßCD (CAPTISOL®) was donated by CyDexInc (Lenexa, United States). Other CDs [HPßCD (mean substitution degree = 4.4), randomly methylated-ß-cyclodextrin (1.6–2.0 methyl unit per anhydroglucose unit; RAMEßCD), hydroxyethyl-ß-cyclodextrin (HEßCD), 2,6-di-O-methyl-β-cyclodextrin (DMßCD), alpha cyclodextrin (αCD) and gamma cyclodextrin (γCD)]] were purchased from Sigma–Aldrich (St. Quentin-Fallavier, France).

All other reagents were of analytical grade from either Merck Eurolab (Fontenay-sous-Bois, France) or Acros organics (Noisy-le-Grand, France) and were used as received.

1.2. Synthesis of phthalimido-ferrocidiphenol (PhtFerr)

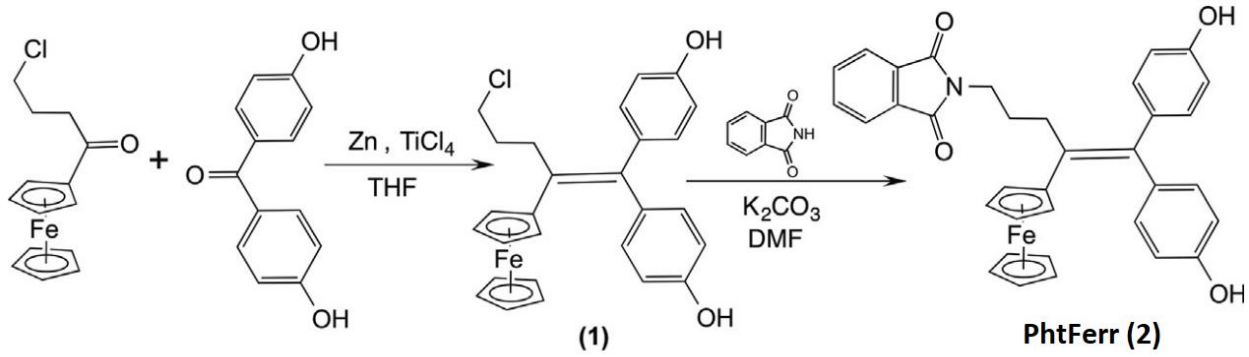

Fig. 2. Synthesis of PhtFerr.

PhtFerr was prepared in three steps. In the first step, the chlorinated ketone was synthesized by the Friedel-Crafts reaction. Then, the chlorinated alkene (**1**) was prepared by the McMurry coupling reaction. Finally, the imide ferrocidiphenol (**2**) was obtained by substitution of the chlorine atom by the phthalimide. The synthesis (Figure 2) was done as follows:

5-chloro-2-ferrocenyl-1,1-bis-(4-hydroxyphenyl)-pent-1-ene (1)

Titanium chloride (11.41 g, 6.6 ml 60.2 mmoles) was added dropwise to a suspension of zinc powder (5.9 g, 90.2 mmoles) in dry THF (500 ml) at 10-20 °C. The mixture was heated at reflux for 2 hours. A second solution was prepared by dissolving 4-chloro-1-ferrocenyl-1-butanone (4.37 g, 15 mmoles) (Elečko et al., 1974), and 4,4'-dihydroxybenzophenone (3.222 g, 15 mmoles) in dry THF (50 ml). This latter solution was added dropwise to the first solution, and the reflux was then continued overnight. After cooling to room temperature, the mixture was stirred with water and dichloromethane. The mixture was acidified with diluted hydrochloric acid until the dark color disappeared and then decanted. The aqueous layer was extracted with dichloromethane and the combination of organic layers was dried on magnesium sulfate. After concentration under reduced pressure, the crude product was

chromatographed on silica gel column with dichloromethane/acetone 90/10 as the eluent and crystallized from dichloromethane, to afford **1** in a yield of 68%, as an orange solid. ^{1}H NMR (acetone-d_6): δ 1.89-2.02 (m, 2 H, CH_2), 2.84 (t, *J* = 8.0 Hz, 2 H, CH_2), 3.54 (t, *J* = 8.0 Hz, 2 H, CH_2), 4.00 (t, *J* = 1.9 Hz, 2 H, C_5H_4), 4.12 (t, *J* = 1.9 Hz, 2 H, C_5H_4), 4.17 (s, 5 H, Cp), 6.74 (d, *J* = 8.7 Hz, 2 H, C_6H_4), 6.86 (d, *J* = 8.7 Hz, 2 H, C_6H_4), 6.90 (d, *J* = 8.7 Hz, 2 H, C_6H_4), 7.10 (d, *J* = 8.7 Hz, 2 H, C_6H_4), 8.29 (s, 1 H, OH), 8.34 (s, 1 H, OH). ^{13}C NMR (acetone-d_6): δ 33.8 (CH_2), 35.1 (CH_2), 46.7 (CH_2Cl), 69.5 (2 CH C_5H_4), 70.6 (5CH Cp), 70.7 (2 CH C_5H_4), 89.1 (C C_5H_4), 116.5 (2 CH C_6H_4), 116.7 (2 CH C_6H_4), 132.0 (2 CH C_6H_4), 132.5 (2 CH C_6H_4), 134.7 (C), 137.6 (C), 138.0 (C), 140.7 (C), 157.5 (2 C). IR (KBr, cm^{-1}): 3433 (OH), 3085, 2951, 2868 (CH, CH_2). MS (CI, NH_3) m/z: 473 $[M+H]^+$. HRMS (ESI, $C_{27}H_{25}ClFeO_2$: $[M]^{+\cdot}$) calcd: 472.0892, found: 472.0887.

***N*-{4-ferrocenyl-5,5-bis-(4-hydroxyphenyl)-pent-4-enyl}phthalimide (PhtFerr) (2)**. A mixture of potassium carbonate (0.69 g, 5.0 mmoles) and phthalimide (0.977 g, 6.6 mmoles), in 100 ml of *N*,*N*-dimethylformamide (DMF) was heated at 80 °C for 15 min. Compound **1** (1.57 g, 3.32 mmoles) was added and the stirring was continued at 80°C overnight. The mixture was allowed to cool to room temperature, poured into diluted hydrochloric acid, and extracted twice with diethyl ether. Then, the organic layer was dried on magnesium sulfate and evaporated under reduced pressure. The residue was purified by flash-chromatography to afford the imide **PhtFerr (2)** that was recrystallized from a diethyl ether/pentane mixture and was obtained as an orange solid with a yield of 83% (1.6 g). mp: 226 °C.^{1}H NMR (acetone-d_6): δ 1.83-1.97 (m, 2 H, CH_2), 2.71 (t, *J* = 8.3 Hz, 2 H, CH_2), 3.62 (t, *J* = 6.8 Hz, 2 H, CH_2N), 3.92 (t, *J* = 1.9 Hz, 2 H, C_5H_4), 4.07 (t, *J* = 1.9 Hz, 2 H, C_5H_4), 4.10 (s, 5 H, Cp), 6.70 (d, *J* = 8.7 Hz, 2 H, C_6H_4), 6.72 (d, *J* = 8.7 Hz, 2 H, C_6H_4), 6.89 (d, *J* = 8.7 Hz, 2 H, C_6H_4), 7.02 (d, *J* = 8.7 Hz, 2 H, C_6H_4), 7.88 (s, 4 H, phthalimide), 8.14 (s, 1 H, OH), 8.26 (s, 1 H, OH). ^{13}C NMR (acetone-d_6): δ 30.6 (CH_2), 33.8 (CH_2), 39.2 (CH_2), 69.4 (2 CH C_5H_4), 70.6 (5CH Cp), 70.7 (2 CH C_5H_4), 89.1 (C C_5H_4), 116.4 (2 CH C_6H_4), 116.5 (2 CH C_6H_4), 124.4 (2 CH phthalimide), 131.8 (2 CH C_6H_4), 132.5 (2 CH C_6H_4), 133.8 (2 C phthalimide), 135.0 (C), 135.7 (2 CH phthalimide), 137.4 (C), 138.0 (C), 140.5 (C),

157.4 (C), 157.5 (C), 169.6 (2 CO). IR (KBr, cm^{-1}): 3429 (OH), 3085, 2944, 2874 (CH, CH_2), 1700 (CO). MS (CI, NH_3) m/z: 584 $[M+H]^+$, 601 $[M+NH_4]^+$. HRMS (ESI, $C_{35}H_{29}FeNO_4$: $[M]^{+\cdot}$) calcd: 583.1446, found: 583.1466.

1.3. Analytical methods for PhtFerr quantification

Determinations of the included ferrocidiphenol were carried out by high performance liquid chromatography (HPLC) or UV-vis spectrophotometry after dissociation by an initial dilution (1%) with pure dimethylsulfoxide (DMSO); the appropriate final adjustments were done with distilled water.

For HPLC determinations, a 20-µl sample was injected into a C_{18} column (5 µm, 4.6×25 cm, Macherey-Nagel, Eckbolsheim, France) using an autosampler (WISP 712, Waters, Guyancourt, France). The mobile phase was a mixture of acetonitrile and water (65/35, v/v) at a flow rate of 1.5 ml/min (SP8800 pump, Spectra Physics, TSP, CA). Detection was performed with a UV spectrophotometer at 286 nm (Waters 490E detector) using a SP-800 integrator (Spectra Physics). The limit of detection (LOQ) was 2.3 mg/l and the limit of quantification (LOQ) was 7.6 mg/l. Standard curves were drawn between 7.8 and 125 mg/l ($r > 0.99$).

1.4. Complexation studies in aqueous phase

1.4.1. Phase solubility studies of PhtFerr complexation

PhtFerr complexation with various CDs was evaluated using the phase-solubility method (Higuchi and Connors, 1965). A suspension of a large excess of phthalimido-ferrocidiphenol (30 mg) in 2 ml of aqueous solutions of the appropriate CD (concentrations ranging from 0.125 to 160 mM, pH adjusted to 7) was stirred in screw-capped amber vials during 24 h on a rock-and-roller agitator at 25 °C. Preliminary time-dependence experiments showed that the equilibrium was reached after this stirring period. Each suspension was then centrifuged at 9000 g for 10 min and diluted from 1/10 to 1/1000 with acetonitrile, and the amount of dissolved PhtFerr was assessed by HPLC at 286 nm.

Phase solubility curves (i.e., solubility of PhtFerr as a function of the CD concentration) were drawn for each CD.

290

1.4.2. UV-visible experiments - Benesi Hildebrand method

First, UV-vis spectra (Carry 50 spectrophotometer, Varian, les Ulis, France) were obtained for a concentration of $2.5.10^{-5}$ M of phthalimido-ferrocidiphenol and various concentrations of CDs (0 to 1.1. 10^{-5} M). RAMEβCD or HPβCD were added and the
295 phthalimido-ferrocidiphenol concentration was kept at $2.5.10^{-5}$ M. All experiments were done in 1% (v/v) DMSO/water mixture (the first dissolution of PhtFerr was done in pure DMSO) to avoid precipitation, and the measurement was taken after 10 min to account for the kinetics of the complex formation.

Then, the mole–ratio titration method was used to calculate the values of the apparent
300 binding constant (Ka) (Benesi and Hildebrand, 1949; Dotsikas et al., 2000; Yoe and Jones, 1944). The experiments were done at various wavelengths obtained from the spectra (low concentration of CD). Another series of experiments was performed with higher CD concentrations (2. 10^{-6} to 25. 10^{-5} M, or high concentration of CD) to confirm the binding constants.

305

1.4.3. ^{1}H-NMR measurements

All experiments were performed on a Bruker Avance DRX-NMR spectrometer operating at 9.4 T (proton frequency: 400.133 MHz) and at a sample temperature of 300 K.

The lyophilized PhtFerr:RAMEßCD complex and pure PhtFerr were dissolved in
310 D_2O:DMSO-d_6 (99:1) adjusted at pD=10.9 with NaOD. This mixture was used for solubility reasons: an alkaline pH can transform phenol in ionized form (phenolates). Chemical shifts were given in parts per million (ppm) relative to the solvent signal (HOD at 4.84 ppm).

2.5. Molecular modeling

Molecular modelling calculations were performed on (and limited to) the well-defined 2,6-di-O-methyl-β-cyclodextrin (DMßCD), by opposition to the undefined randomly substituted-ß-cyclodextrins, using the program Spartan14 (Wavefunction Co., Irvine, CA, USA). After building the CD model, an energy minimisation was carried out using the Merck molecular force field (MMFF) method. The PhtFerr molecule was then edited in the same window, and a short energy minimisation was then carried out (MMFF method). To evaluate the affinity of each of the 4 substituents of the alkene double bond for the DMßCD, the calculations where performed to a 1:1 PhtFerr:DMßCD ratio (Table 1, entries 1-4). The file was thus duplicated in 4 files. In each of the files, the PhtFerr molecule was oriented in a way where each of the 4 moieties of the double bond (one moiety tested per file: ferrocenyl, phthalimidylpropyl, phenol #1 -*cis* with the ferrocenyl- and phenol #2) were moved closer to the entry of the CD, approximately in its axis.

For each, an energy minimisation was then carried out using the Merck molecular force field (MMFF) method, and the geometry was then optimized using the semiempirical PM3 quantum-mechanical method. Semiempirical PM3 quantum-mechanical methods were used to determine the affinity of PhtFerr with the CD. This requires calculation of the energies of the (PhtFerr-CD) group, of the CD itself, and of PhtFerr, the latter two in the conformations they had in the molecular assemblies to give the $\Delta r H°$ enthalpy variations of the reactions: PhtFerr + CD →molecular assembly.

In the case of a 1:2 **PhtFerr**/CD inclusion complex, we can suppose that one of both CDs (CD1) make an inclusion complex with the ferrocenyl moiety, due to its better affinity, and thus, we limited the calculations to three possibilities (entries 5-7). The file of entry 1 was copied 3 times, and in each copy, a second CD (CD2) was placed in forced inclusion for each of the 3 other substituents. For each, an energy minimisation was then carried out using the Merck molecular force field (MMFF) method, and the geometry was then optimized using the semiempirical PM3 quantum-mechanical method. Semiempirical PM3 quantum-mechanical methods were used to determine the affinity as before. This required calculation of the energies of the reactions: **PhtFerr** + CD1 + CD2 →molecular assembly (Table 1, entries 5-7).

The same procedure was used for the calculations with 3 CD (Table 1, entries 8-9).

Table 1

Calculations of PhtFerr with inclusion of each of its substituents into 1CD separately (entries 1–4), combination with 2CD (one inclusion being with the ferrocenyl group, entries 5–7) and inclusion with 3CD (at least with ferrocenyl and phthalimidyl groups, entries 8–9). Inclusions were done by the wide side of the CD, except for the values between parentheses where inclusion were done by the narrow side of the CD.

Entr	Ferrocenyl	Phenol #1	Phenol #2	Phthalimidyl	$\Delta_r H^o$ (kJ/mol) wide (narrow)
1	CD				-52 (-83)
2		CD			-26 (-34)
3			CD		-27 (-30)
4				CD	-38 (-33)
5	CD1	CD2			-93 (-113)
6	CD1		CD2		-92 (-73)
7	CD1			CD2	-83 (-108)
8	CD1	CD2		CD3	-134 (-134)
9	CD1		CD2	CD3	-106 (-135)

2.6. Solid phase analysis of PhtFerr:RAMEβCD

To obtain a lyophilized sample, an excess of PhtFerr (30 mg) was stirred (25 °C; 24 h) in distilled water (2 ml) containing 160 mM of RAMEßCD or HPßCD and filtered through a 0.22 µm membrane filter (Millipore HA). The filtrate was freeze-dried and stored at +4 °C until use. The complexation efficiency of PhtFerr was determined by HPLC as previously described.

The solid phase analysis of the complexes was performed on these lyophilized samples.

2.6.1. X-ray diffraction (XRD)

The PXRD measurements were performed using a PanalyticalX'Pert Pro diffractometer equipped with a Cu tube, a Ge(111) incident-beam monochromator (λ = 1.5406 Å) and an X'Celerator detector. Data collection was carried out in the scattering angle range 3-70° with a 0.0167° step over 90 min.

2.6.2. Differential scanning calorimeter (DSC)

The DSC thermograms were obtained on a scanning calorimeter (DSC Q10, TA Instruments). The instrument was calibrated at various temperatures before starting the procedure. Each sample weighed 5 mg and was heated in sealed aluminum pans under nitrogen environment at 50 ml/min. The limit of detection was controlled from 10 °C to 300 °C and the ramp was 10 °C/min.

2.7. Pharmaceutical properties of the PhtFerr:RAMEβCD complex

2.7.1. Dissolution and diffusivity across a dialysis membrane

To investigate the dissolution, an amount (5 mg) of the lyophilized PhtFerr:RAMEβCD complex was suspended in water. The suspension was incubated at 25 °C in a shaking-bath (200 strokes/min, Heito, France). Aliquots (1 ml) were taken at various time intervals up to 24 h and centrifuged (7200 g, 5 min, Denver Instruments, MA). Each supernatant was analyzed by HPLC to assess the drug contents. The results are presented as mean±SD of triplicate experiments.

A dialysis was also realized. The bag (cut-off: 14 000 daltons) contained an aqueous solution of 5 mg/2 ml of PhtFerr:RAMEβCD, and 498 ml of distilled water was added under magnetic stirring. Aliquots were taken and analyzed as previously described.

2.7.2. Cell culture: *in vitro* cytotoxicity on U87 cell lines

The cytotoxic activity of PhtFerr and the PhtFerr:RAMEβCD complex was tested on glioblastoma cell lines (U87).

The concentration of PhtFerr and PhtFerr:RAMEβCD required to induce a decrease in cell viability was assessed by determining the ability of the U87 cells to reduce the tetrazolium dye (MTT). The assay is based on the reduction of the MTT, by mitochondrial succinate dehydrogenase to a colored, soluble formazan complex, which is quantified spectrophotometrically at 560 nm (Hansen and Nielsen, 1989).

The U87 suspension was seeded in 96-well culture plates with 100 µl of medium (5. 10^3) per well. After 12 hours, varying amounts of PhtFerr and PhtFerr:RAMEβCD, ranging from 10^{-3} to 10^{-9} M, were added to the wells, and the culture plates were incubated for 72 h at 37 °C. For the MTT assay, 100 µl of MTT (5 mg/ml stock solution in phosphate-buffered saline, PBS) was added to each well and cells were incubated for 3 h at 37 °C. Viable cells convert the soluble yellow MTT to insoluble purple formazan by the action of mitochondrial succinate dehydrogenase. A 100 µl volume of dimethylsulfoxide (DMSO) was added to dissolve the formazan crystals. The optical density was measured at 560 nm with a microplate reader. The absorbance is proportional to viable cell number, and survival was calculated as the percentage of the staining values of the untreated cultures.

2.7.3. Hemolytic activity

Hemolytic activity of the protein was tested using erythrocytes from a human source. Freshly collected blood samples were immediately mixed with an anticoagulant (Alsever's solution, pH 7.4) to prevent blood coagulation. To obtain a pure suspension of erythrocytes, 1 ml of whole blood was diluted to 20 ml in phosphate buffered saline (PBS, pH 7.4), and centrifuged at 250 g for 5 min at 4 °C. The supernatant and buffy coats were removed by gentle aspiration, and the above process was repeated two more times. Erythrocytes were finally re-suspended in PBS to obtain a 1% solution for hemolytic assay. For this, various concentrations of PhtFerr and PhtFerr:RAMEβCD (0.05–1 mg/ml) were added to the suspension of red blood cells. The PhtFerr and PhtFerr:RAMEβCD–erythrocyte mixtures were incubated at 37 °C for 1 hour in water bath and then centrifuged at 250 g for 5 min at 4 °C. The absorbance of the supernatants was determined at 545 nm to measure the extent of red blood cell lyses. Positive control (100% hemolysis) and negative control (0% hemolysis) were also run by incubating erythrocytes in PBS containing 1% Triton X-100 and PBS alone, respectively (Malagoli).

3. Results and discussion

PhtFerr is very lipophilic and has a complex structure with 4 main moieties (i.e., 3 aromatic rings and a ferrocene) that could be included in the cavity of CDs (Figure 1). A recent study demonstrated that hydroxyferrociphenol could be complexed by methylated CDs (Buriez et al., 2008). These experiments were done by cyclic voltammetry, which allows quantifying a strong interaction with the organometallic. The complexation has been attributed to the very hydrophobic ferrocenyl moiety. In other circumstances, phenol groups have also been described to be able to interact with CDs in many compounds (Chelli et al., 2007), and the phthalimidyl-group, which is also hydrophobic, is another candidate for complexation. This particular structure makes the study difficult, but we were able to propose a possible structure for each complex coexisting in solution using phase solubility studies, UV-visible experiments, ^{1}H-NMR studies and a molecular modeling approach.

3.1. Phase solubility studies of PhtFerr

The first experiment, which is usually done to test the dissolving properties of the complexation, is the phase solubility study first described by Higuchi and Connors in 1965 (Higuchi and Connors, 1965).

In our experiment (Figure 3), αCD did not significantly improve the solubility of PhtFerr; this is probably due to the lack of incorporation of the PhtFerr in the small cavity of αCD (internal diameter: 0.57 nm). However, methylated β-cyclodextrins (RAMEßCD and DMßCD), which have an internal diameter of 0.68 nm, showed significant solubilization properties: the curve exhibited a positive curvature described as Ap-type by Higuchi (Higuchi and Connors, 1965) (Figure 3). This type of curve is observed if more than one CD can complex the drug corresponding to 1:2,1:3,1:4 (or more) stoichiometries. The determination of the binding constant can be performed for up to 1:2 complexes (Alfonsi et al., 2013), but the combinations of 1:2 complexes and even higher stoichiometries are possible for PhtFerr complexes. We consider that the determination of the binding constant by this method would be unreliable.

Nevertheless, the phase solubility studies allowed us to select the PhtFerr:RAMEßCD for further experiments. The PhtFerr:HPßCD complex was studied for comparison.

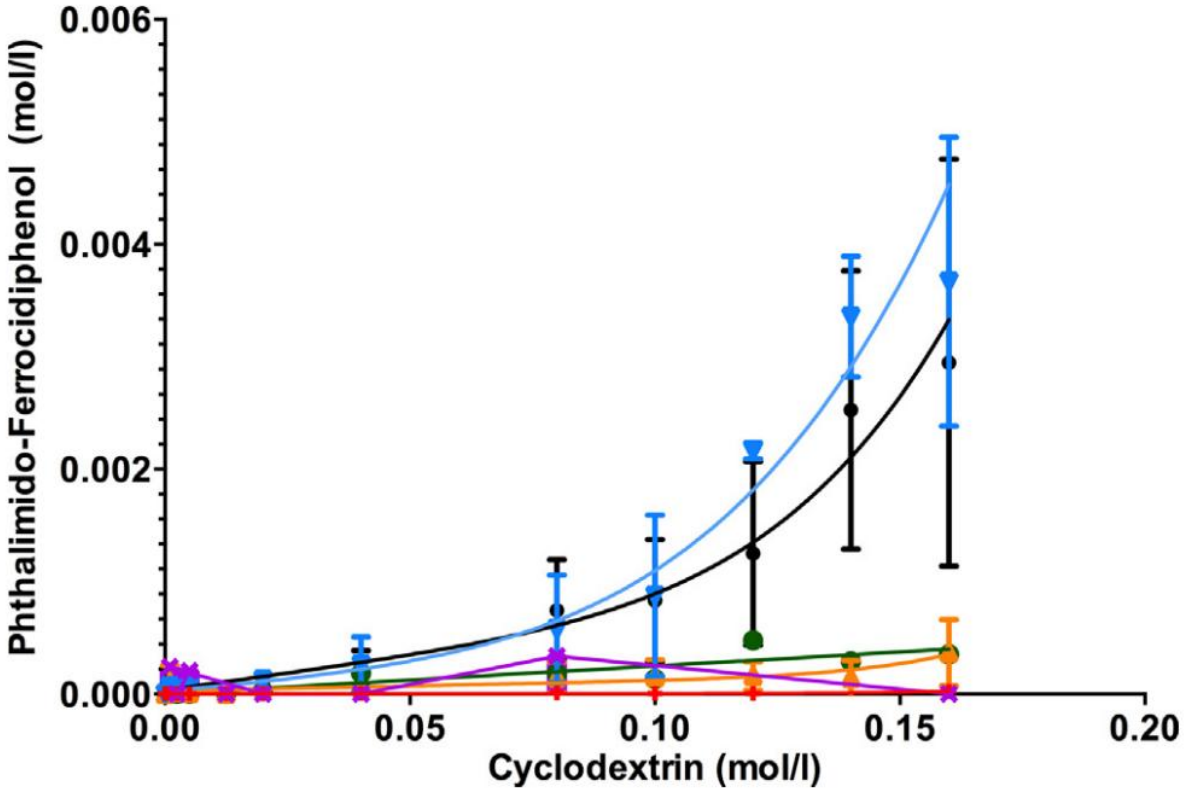

Fig. 3. Phase solubility diagrams of PhtFerr in the presence of αCD(–+–), RAMEβCD (-●-), DMßCD (–▼–), HPβCD (–▲–); HEβCD (–■–), SBEßCD (–■–) and γ-CD (–●–).

465

3.2. Molecular modeling

Calculations for a 1:1 PhtFerr:CD ratio:

For the four moieties, binding to the CD (wide side) is thermodynamically favoured, as
470 evidenced by the modest but negative enthalpies of formation for the **PhtFerr**-CD assemblies. The most negative value for the ferrocenyl moiety (-52 kJ/mol, Table 1) shows clearly its best affinity for the CD compared to the other moieties. This is due to hydrophobic interactions between the cyclopentadienyl rings and the methoxy groups

(Buriez et al., 2008). The orientation of the ferrocenyl group in the CD is neither parallel nor perpendicular to the molecular axis of the CD. Instead, it is intermediate due to the hindrance of the others moieties. The affinity of the CD for the phthalimidopropyl group (-38 kJ/mol) is the second best one, followed by quite similar affinities for phenyl groups #1 and #2 (-26 and -27 kJ/mol, respectively). For all of these inclusions, one of the phenol group forms a hydrogen bond between its hydrogen atom and an oxygen atom of the CD.

For comparison, entering the moieties by the narrow side of the CD was also calculated. Again, the ferrocenyl group had the best inclusion affinity, and its absolute value increased, as for both phenyl groups (even though no hydrogen bond was formed with one of the phenol groups for these three inclusions). However, the affinity slightly decreased for the phthalimidopropyl group, even though a hydrogen bond exists with phenyl group #2.

Calculations for a 1:2 PhtFerr:CD ratio:

The 1:2 systems (wide side and narrow side) are the most favored in comparison to 1:1 systems, but their energies differences are quite small. Therefore, there is a possible competition between all of these systems and the presence of a complex mixture where inclusions with two CDs, one being with the ferrocenyl group, predominate. This should be increasingly complex because of the possibility of inclusion by the narrow side of the CD too and wide side – narrow side mixtures. For example, calculations for inclusion by the narrow sides of two CD (one being with the ferrocenyl group) gave the best affinity for inclusion of the phenyl groups #1 and the phthalimidylpropyl group in comparison to inclusion by 2 wide sides of CDs (entries 5 and 7).

The case of inclusion of the ferrocenyl and the phthalimidopropyl moieties by the wide side of the CD, selected as an example (Supplementary Figure 1), shows that the four moieties of **PhtFerr** are influenced by the inclusion. Indeed, in addition to the inclusion of ferrocenyl and phthalimidylpropyl moieties, each of the two phenol groups makes a hydrogen bond with a CD. We can see that the ferrocenyl group is nearly perpendicular to the molecular axis of the CD.

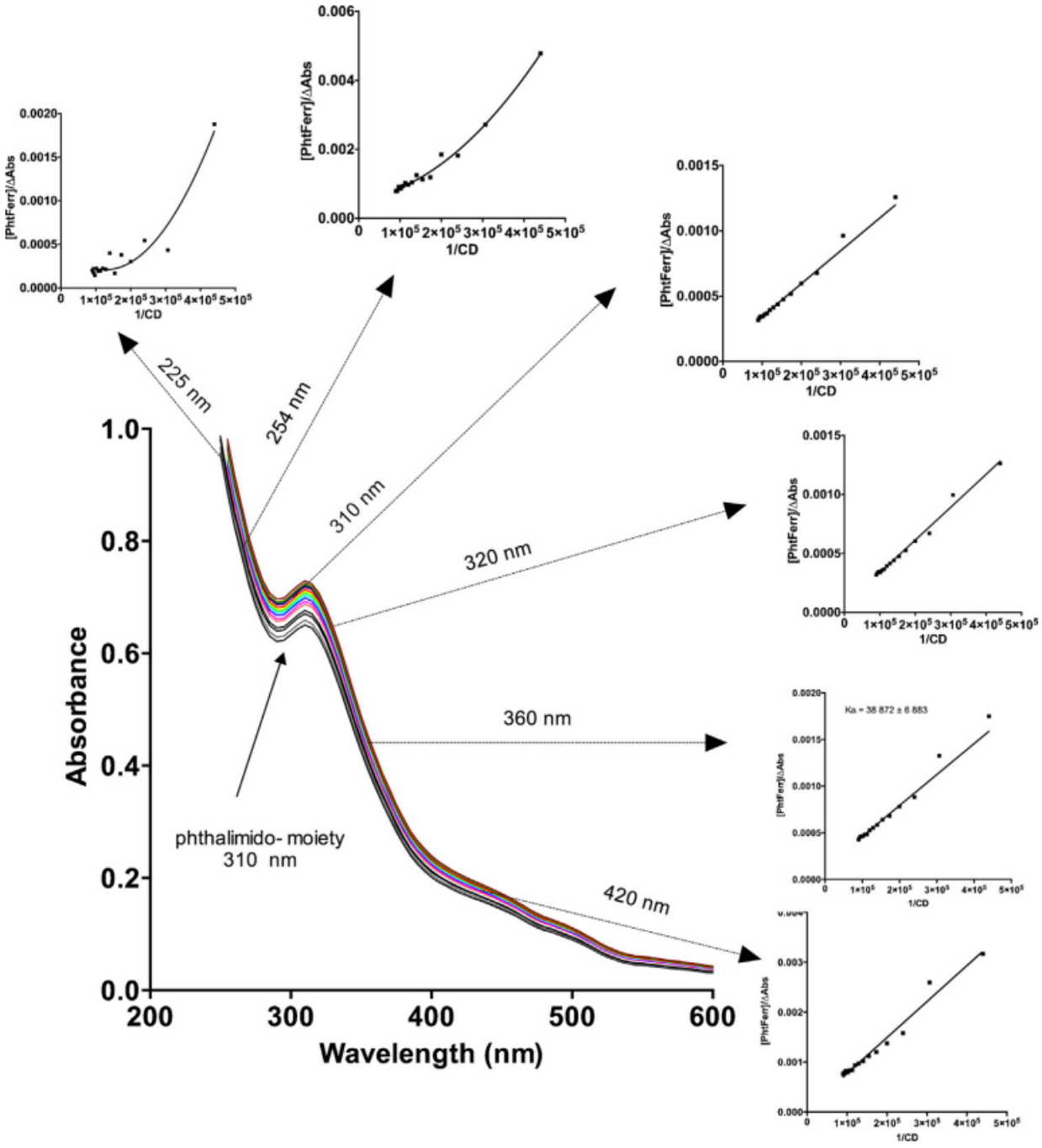

505

Fig. 4. Spectra of PhtFerr (2.5 X10^{-5}M). The first spectrum (i.e. the lower curve) was obtained in water with 1% DMSO. The addition of various amount of RAMEßCD produced a hyperchromic effect especially at 310 nm. Insets: Benesi–Hildebrand plots for the complexation PhtFerr in RAMEßCD. The formation of the complex(es) was monitored at various wavelengths from the spectra data.

510

Calculations for a 1:3 **PhtFerr** :CD ratio:

Although the affinities are better than for the 1:1 or 1:2 ratios, the modeling (Table 1, entries 8-9) shows that the steric hindrance of the CD makes the moieties in a less deep inclusion inside the CD. These values could be more an indication of the clustering effect of the CD than of the inclusion and could be not very relevant.

3.3. UV-visible experiments

In further experiments, we tried to confirm the various hypotheses deduced from the molecular modeling, but our major concern was the insolubility of the PhtFerr in aqueous media. Consequently, the introduction of 1% DMSO was necessary to dissolve PhtFerr and reach detectable concentrations. This can lead to variations compared to the results that would be obtained in pure water. Hence, the binding constant must be considered as “the binding constant in 1% DMSO.”

In 1% (v/v) aqueous DMSO solution, PhtFerr exhibited a typical spectrum. The λ_{max} of the phthalimidyl group is at 310 nm mainly due to the conjugation of the maleimide ring with the benzene nucleus (Supplementary Figure 1). The phenol groups are known to produce a λ_{max} of approximately 270 nm and correspond to the left part of the spectrum. The λ_{max} of the ferrocenyl moiety is approximately 200 nm in various solvents (Scott and Becker, 1961) and can impact the spectrum mainly below 250 nm. Another minor peak of absorbance is usually observed at approximately 445 nm for ferrocene derivatives, but this peak was undetectable in our conditions.

After addition of various amounts of CD (Figure 4), the spectrum shows an important concentration-dependent hyperchromic effect at 310 nm, likely corresponding to the complexation of the RAMEßCD with the phthalimidyl moiety. Double reciprocal Benesi-Hidebrand plots ([PhtFerr]/ΔAbs *vs*. 1/[CD]) were first drawn with the spectra data obtained at 310 nm, fitting a linear regression model (R>0.99) (Figure 4, inset). This wavelength of 310 nm corresponds to the maximum of absorbance of the phthalimidyl group, but a significant absorbance due to phenol groups can still be

present. To limit this problem, the experiment was repeated at higher wavelengths (i.e., 320, 340, 360, 380, 400 and 420 nm; Figure 4, insets). In our first hypothesis, we assumed that the phthalimidyl group is the only one that can possibly have an impact on the absorbance between 340 and 380 nm. Nevertheless, the curves were linear (R>0.99) between 310 and 400 nm, leading to a similar apparent binding constant (Table 2).

Table 2

Apparent binding constants obtained by the modified Benesi-Hildebrand method.

Wavelength	Apparent binding constant (K_a)—M^{-1}	*R*
310	36,959 ± 4894	0.9964
320	32,150 ± 5665	0.9953
340	36,310 ± 4738	0.9969
360	38,433 ± 6159	0.9949
380	30,440 ± 8687	0.9941
400	34,328 ± 7674	0.9918
420	33,534 ± 9622	0.9467

In the phase solubility study, PhtFerr:RAMEßCD has been demonstrated to be at least a 1:2 complex; hence, it is necessary to explain why we have an apparent 1:1 interaction deduced from the Benesi Hildebrand plots.

As previously mentioned, between 310 and 400 nm, the variation of absorbance is only due to the interaction on the phthalimidyl moiety, and this phenomenon allowed us to isolate the interaction with this group in the spectra. This is a highly unusual situation in the field of CD, which can interact with several aromatic groups in the same molecule, but these aromatics are usually the same (i.e., 2 phenols (Chalumot et al., 2009)) or have very similar UV absorbances (i.e., para chloro- *vs*. ortho chloro- (Alfonsi et al., 2013)).

To find the equation that is related to the 1:1 apparent constant that we observed, we have to take in account the interaction with multiple complexes already in the solution. All of the “starting compounds” (Figure 5) include PhtFerr and various complexes, but we had to exclude the complexes showing an interaction with the phthalimidyl group;

hence, we can assume that the molar absorption coefficient of these starting compounds is similar to that of PhtFerr between 310 and 400 nm. These complexes are named PhtFerr:$(CD_0)_n$ (Figure 5); each CD_0 corresponds to a CD that does not interact with the phthalimidyl group.

On the contrary, the final compounds are the corresponding complexes that interact with the phthalimidyl group (PhtFerr:$(CD_0)_n$:**CD_{Pht}**, Figure 5); the molar absorption coefficient at 310 – 400 nm of all these compounds (i.e., of the phthalimidyl group) is modified by the complexation.

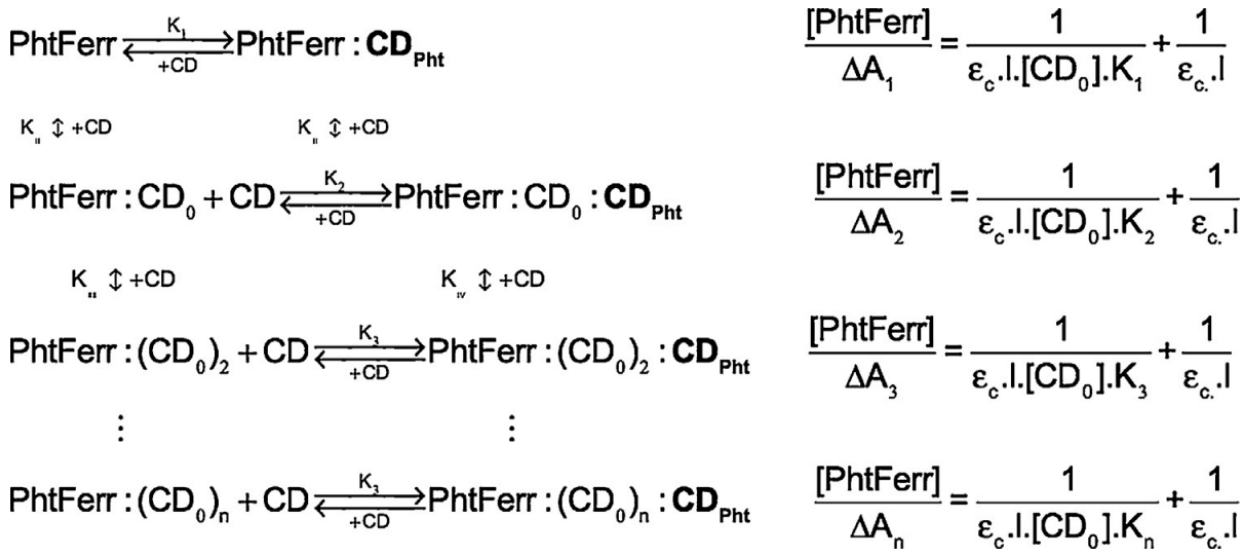

Fig. 5. Complexation of the phthalimidyl moiety (on the left) and corresponding Benesi–Hildebrand equations (on the right). The wavelength has to be chosen to get a variation of absorbance only due to the interaction with the phthalimidyl group. We also assume that the molar absorption coefficient is the same for each Pht:$(CD_0)n$:CDPht complex.

The corresponding Benesi Hildebrand equations are given in Figure 4, and the sum of these equations gives:

$$[\mathrm{PhtFerr}].\sum_{n}^{i=1}\frac{1}{\Delta A_i} = \frac{1}{\varepsilon_c.l.[CD_0]}.\sum_{n}^{i=0}\frac{1}{K_i} + \frac{n}{\varepsilon_{CompPht}.l} \qquad \text{(Eq.1)}$$

Therefore,

$$[\mathrm{PhtFerr}].\frac{\sum_{n}^{i=1}\frac{1}{\Delta A_i}}{n}=\frac{1}{\varepsilon_c.l.[CD_0]}.\frac{\sum_{n}^{i=0}\frac{1}{K_i}}{n}+\frac{1}{\varepsilon_c.l} \qquad \text{(Eq.2)}$$

The harmonic mean can be used to find average speeds. This has been described, for example, for agglomeration and aggregation processes (Gadomski and Ausloos, 2006). For a method of calculation of average speeds, see Gadomski et al. (Gadomski and Ausloos, 2006; Gadomski et al., 2007; Gadomski et al., 2005).

Here, the observed variation of absorbance ΔA is the harmonic mean of the ΔA_i of each complexation reaction ($\Delta A=\frac{n}{\sum_{n}^{i=1}\frac{1}{\Delta A_i}}$) and the apparent binding constant K_a can also be defined as a harmonic mean ($K_a=\frac{n}{\sum_{n}^{i=1}\frac{1}{K_i}}$).

Therefore, Eq.2 gives:

$$\frac{[\mathrm{PhtFerr}]}{\Delta A}=\frac{1}{\varepsilon_c.l.[CD_0].K_a}+\frac{1}{\varepsilon_c.l} \qquad \text{(Eq.3)}$$

The equation is similar to the Benesi Hildebrand equations and is linear for [PhtFer]/ΔA as a function of 1/[CD_0]. Consequently, we can confirm that the linear curves obtained for double reciprocal curves of Benesi-Hildebrand correspond to a 1:1 apparent complexation with the phthalimidyl group. The apparent binding constant (K_a, Table 2) is a harmonic mean value of various K_n due to the interaction with several complexes. Between 310 and 420 nm, the variation of the wavelength does not have an effect on the results (Table 2).

Because the spectra have been obtained with relatively low concentration, the same experiment has been repeated at a higher concentration of CD (Supplementary Figure 2), and similar results have been obtained with a K_a of 34 237 ± 7 905 M^{-1}. These results allow us to propose an apparent binding constant (K_a) of approximately 34.10^3 M^{-1} in 1% DMSO.

It is of note that 1:2 complexes have already been studied with mole titration methods (Chalumot et al., 2009). Nevertheless, in each case, both guest moieties are symmetrical, with similar molar absorption coefficients for both moieties. Consequently, ΔA can be used to study a global effect of both interactions.

For example, Chalumot et al. have complexed polyaromatic compounds (naphthalene, fluorine, biphenyl, and phenanthrene) that can give symmetrical 1:2 complexes. In this specific case, modified Benesi-Hildebrand plots do not follow a linear regression but can be fitted with the quadratic equation:

$$\frac{[\text{Drug}]}{\Delta A} = \frac{1}{\varepsilon l [\text{CD}]^2 K_\alpha} + \frac{1}{\varepsilon l} \quad \text{with} K_\alpha = K_{1:1} \times K_{1:2} \qquad \text{(Eq.4)}$$

The interaction with both phenol groups of PhtFerr [$\text{PhtFerr}:(\text{CD}_0)_n + 2\text{CD}_0 \rightleftarrows \text{PhtFerr}:(\text{CD}_0)_n:(\text{CD}_{\text{Phenol}})_2$] probably has a role in the quadratic curves that we observed at 254 nm and below. The demonstration would follow the same demonstration but this time with a quadratic function and the apparent K_α would be the medium value of various $K_{\alpha n}$. Nevertheless, the absorbance of the ferrocenyl and phthalimidyl groups at 254 nm is possible, and we consider that the determination of K_α is not possible.

The use of HPßCD for the solubilisation of PhtFerr is less efficient (Supplementary Figure 3); nevertheless, a low amount of PhtFerr could be dissolved. The spectra (Suplementary Figure 3) show that the variation of absorbance is much lower at 310 nm. This is consistent with the results obtained with NMR and phase solubility studies. Due to the low variation of absorbance between 310 and 420 nm, it was not possible to draw meaningful curves.

Table 3 ^{1}H NMR chemical shifts (δ) of free and complexed phthalimido–ferrocidiphenol

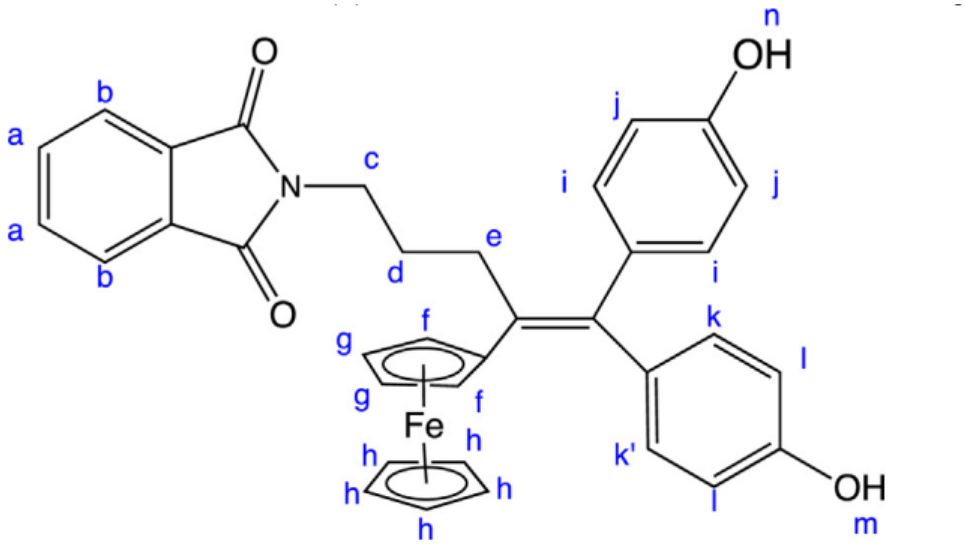

	PhtFerr	PhtFerr:RAMEßCD	$\Delta\delta^{a}$
a,b (phthalimide)	7.453	7.418	−0.035
c	3.210	ND	–
d	ND	ND	–
e	1.710	1.749	0.039
f,g (ferrocene)	4,075	ND	–
g,h (ferrocene)	4.115	4.118	0.003
i,k (phenol)	6.402	6.285	−0.117
j,l (phenol)	6.499	6.510	0.011
m	–	–	
m	–	–	

[a] $\Delta\delta = \delta(\text{complex}) - \delta(\text{free})$.

3.4. ^{1}H-NMR experiments

NMR spectrometry is known to be one of the most useful methods to obtain information about the geometry of inclusion complexes. Nevertheless, the solubility of PhtFerr is too low in D_2O to reach the limit of detection. Consequently, the use of low concentrations of DMSO-d_6 was necessary in this experiment. In a first attempt, we dissolved each compound in 1% of DMSO-d_6, but even in these conditions, the concentration of PhtFerr was too low. The only solution was to use also an alkaline solvent (NaOD, pD = 10.9) to transform phenol in phenolate and to obtain a more soluble form of PhtFerr. The results are presented in table 3 where the corresponding shifts are $\Delta\partial=\partial$(complex)-∂(free). In

the presence of the CD, phenols H_i and H_k protons are strongly up field shifted (Table 3). The partial spectrum corresponding to the aromatic peaks (phenols and phthalimidyl) is shown in Figure 6. Lower shifts are observed for the other aromatic protons (i.e., phthalimidyl and ferrocenyl groups), confirming an interaction with these groups.

Small new peaks were also observed in the aromatic area (Figure 6), and this was attributed to the detection of a degradation of the phthalimidyl group at pD = 10.9. When the experiment is done immediately after the addition of the basic solvent, the degradation is negligible and does not impact the other peak of the spectrum.

Another drawback of this experiment is the transformation of phenols in phenolates at pD 10.9. This can significantly impact the interaction with the phenol groups. Nevertheless, phenolates are more hydrophilic than non-ionized phenols, and the interaction should be weaker. Hence, our experiment is in favor of an interaction of the RAMEßCD with the phenol of the PhtFerr. The interaction of the RAMEßCD with the ferrocenyl and the phthalimidyl groups is also confirmed.

Due to the degradation of the molecule, it was not possible to do 2D experiments and obtain accurate information on the conformation.

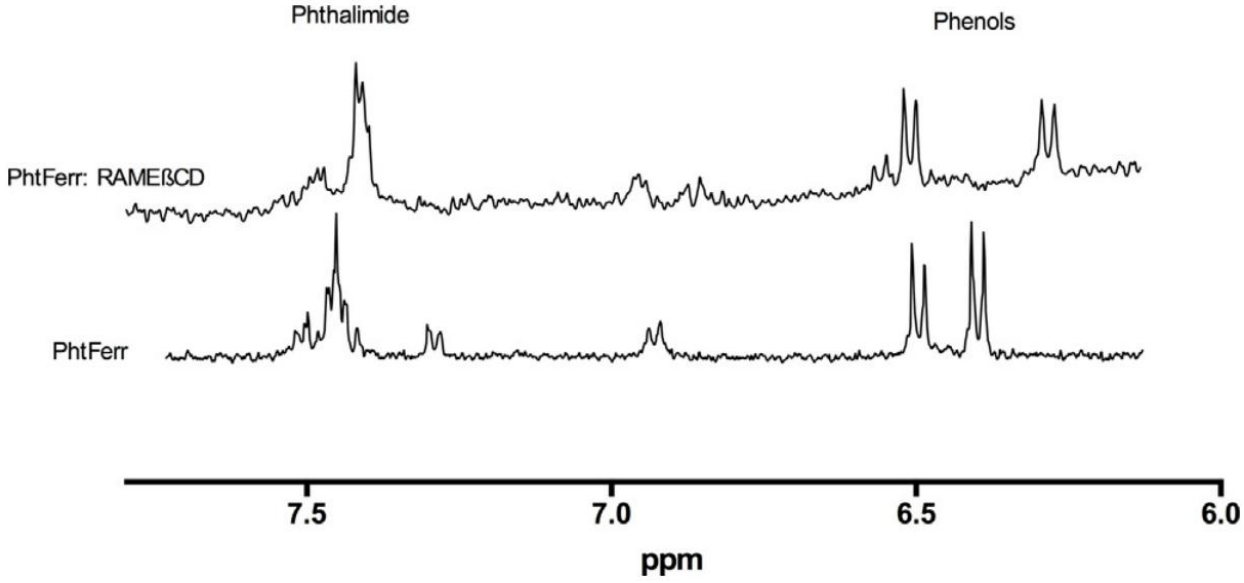

Fig. 6. Partial ^{1}H-NMR spectra of RAMEβCD/PhtFerr and pure PhtFerr in D_2O: DMSO-d_6 (99:1) at pD = 10.9 corresponding to the aromatic ring part (phenols and phthalimidyl).

3.5. **Solid phase analysis**

The solid phase analysis of the complexes was performed on these lyophilized samples (frozen overnight at -20 °C and freeze-dried in a SMH15 freeze-drier (Usifroid, Maurepas, France). The concentration of PhtFerr determined by HPLC was 3.51± 0.10 mg/g.

The DSC and XRD are widely used to study the complexation of this kind of compound. In fact, these analytical methods were used to ascertain the inclusion process in solid complexes obtained by freeze-drying.

The DSC profile (Figure 7) of pure RAMEβCD exhibited a large endothermic event from 90 to 140°C, attributed to the evaporation of the absorbed water, whereas the melting point of PhtFerr occurred at 216°C. The DSC profile of the two raw materials, compared to the thermogram of the PhtFerr:RAMEβCD, confirms that there was a real inclusion of the PhtFerr into the RAMEβCD; the formation of an inclusion complex is suggested by the absence of both melting endotherms in the DSC thermogram of the complex. This was already described for other drugs, such as melarsoprol (Gibaud et al., 2005) or zolpidem (Trapani et al., 2000).

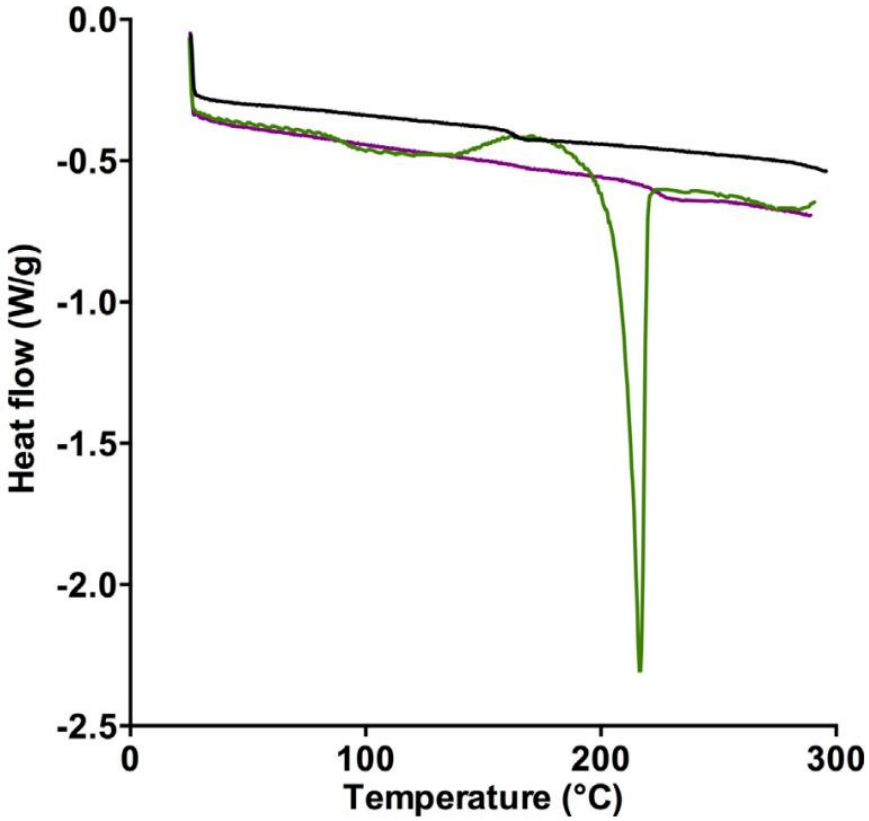

690 **Fig. 7.** DSC curves for PhtFerr, PhtFerr:RAMEβCD and RAMEβCD.

The XRD (Figure 8) also demonstrated the formation of an amorphous inclusion complex between RAMEβCD and PhtFerr. The diffractogram of pure PhtFerr exhibited numerous peak characteristics of its crystalline form, its high and rising background is
695 due to fluorescence as iron present in PhtFerr fluoresces in the X-rays produced by a copper target (Tahri et al., 2012). RAMEβCD showed only a broad amorphous band.

The diffraction pattern of PhtFerr:RAMEßCD shows no Bragg peaks as the compound is amorphous. Furthermore, no sign of crystalline PhtFerr is present in the complex. PhtFerr is present but it has lost its crystalline state and may be present as isolated
700 molecules.

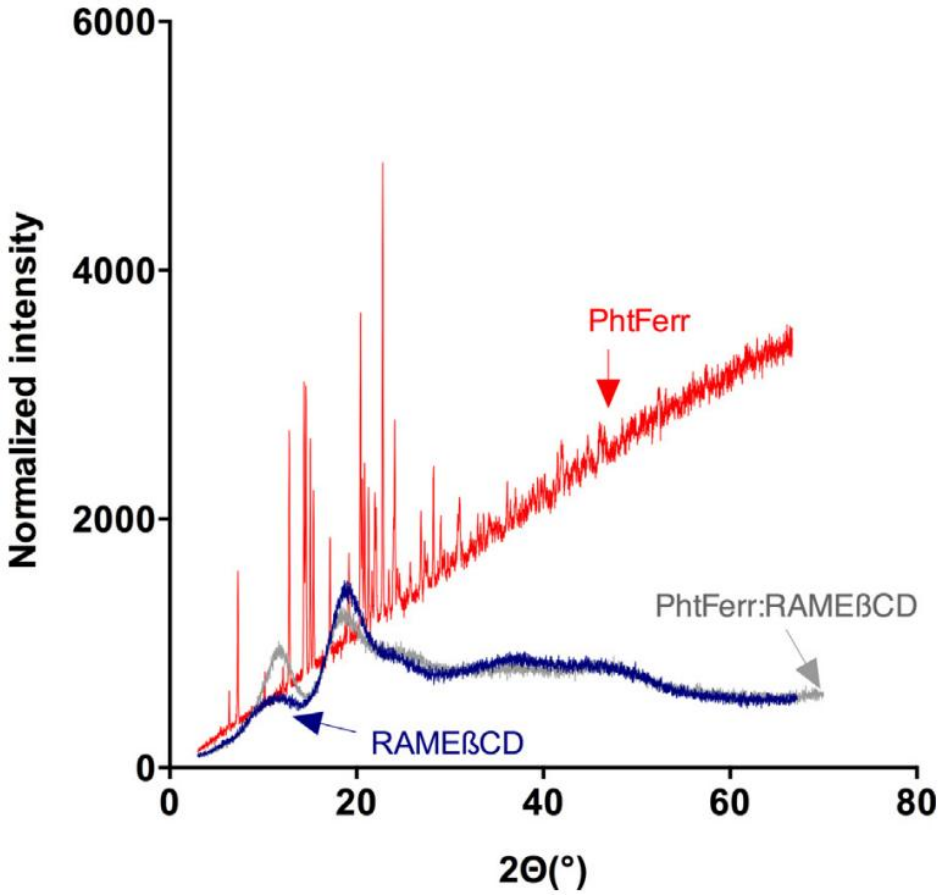

Fig. 8. XRD diffraction spectra of PhtFerr, PhtFerr:RAMEβCD and RAMEβCD.

3.6. **Pharmaceutical properties**

3.6.1. **Dissolution and diffusibility studies of PhtFerr:RAMEβCD and HPβCD complexes**

The aim of this work was to develop a soluble formulation of PhtFerr. Therefore, the dissolution profile and the diffusibility are key pharmaceutical parameters. An immediate dissolution of PhtFerr:RAMEßCD was observed in water (100%). However, pure PhtFerr cannot be dissolved and was not detectable. Another experiment was realized in a dialysis bag to take into account the diffusibility properties of the complex. Figure 9 illustrates the dissolution profile obtained with PhtFerr:RAMEβCD. The diffusion of the complex through the dialysis membrane was quite slow, but more than 70% are in the external phase after 8 h.

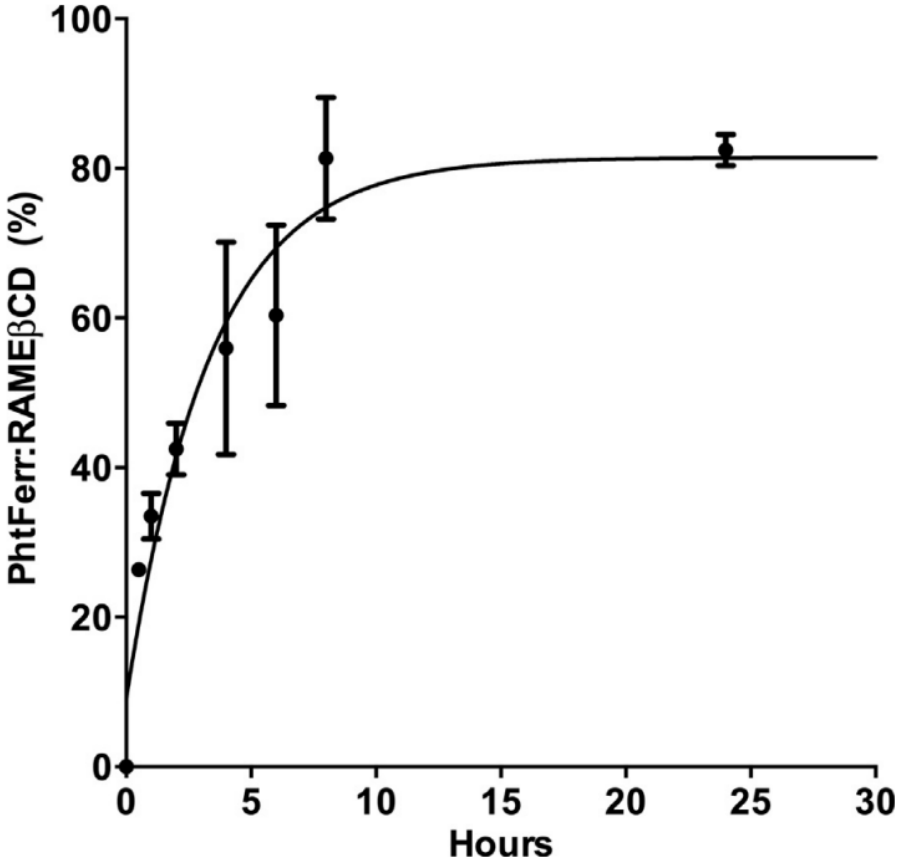

Fig. 9. Dialysis of PhtFerr:RAMEβCD in a dialysis bag (final concentration : 5 mg/ 500 ml)—cutoff 14,000 Da.

3.6.2. *In vitro* cytotoxicity of PhtFerr:RAMEβCD for U87 cell lines

In vitro cytotoxicity of PhtFerr:RAMEβCD for U87 cell lines (Figure 10) was very low, indicating a very good cytotoxic activity compared to the Fc-diOH (IC_{50} = 0.5 µM) (unpublished work). Moreover, the growth inhibition of cells exposed to PhtFerr:RAMEβCD (0.028 ± 0.007 µM) was similar to that of the free PhtFerr (0.018 ± 0.003 µM). The slightly higher value of PhtFerr:RAMEβCD could be explained by the protection of the ferrocenyl moiety, which is considered as the pharmacologically active group (Hillard et al., 2010; Jaouen and Top, 2013). Our results suggest that the complexation of PhtFerr by RAMEβCD does not impair its pharmacological activity. Hence, the CDs complexes of PhtFerr are good candidates for the treatment of glioma.

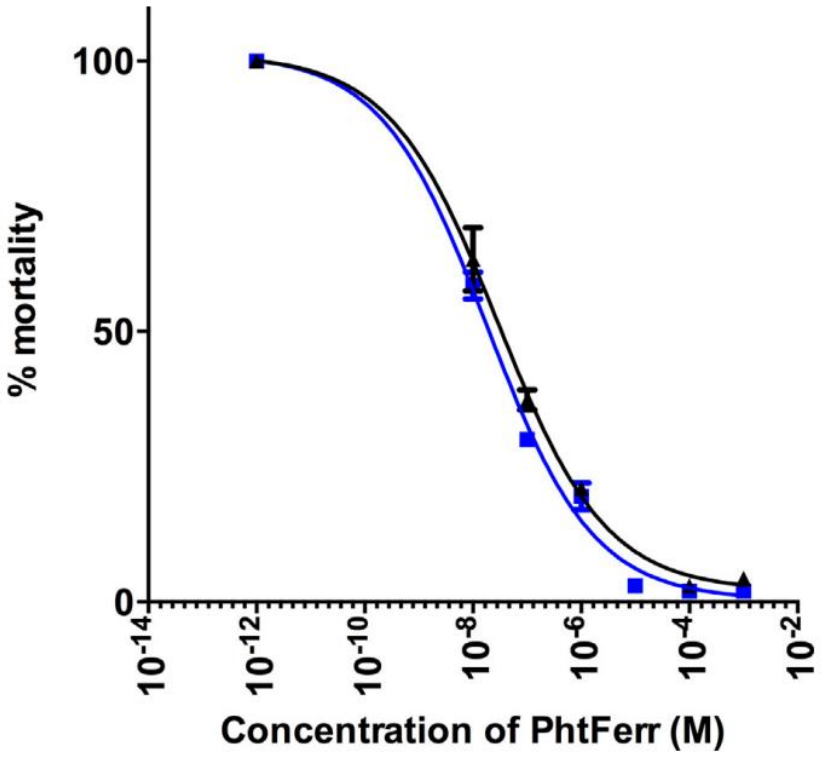

Fig. 10. Cytotoxicity of PhtFerr (-▲-) and PhtFerr:RAMEßCD(-■-): representative cytotoxicity dose response curves.

735

3.5.3. Hemolytic activity

Methylated CDs are known to have hemolytic properties (Jodál et al., 1988).

The comparison of hemolytic properties between the free drug and the complex is necessary before any injection. In our experiment, PhtFerr:RAMEßCD was slightly more
740 hemolytic than PhtFerr (Figure 11), but in any case, the maximal concentration leading to the absence of hemolytic activity was 10 µM. This concentration is high compared to the IC_{50} (0.028 ± 0.007 µM), and we consider that an intravenous administration is possible.

An oral administration is also possible with this kind of complex, but the intestinal
745 absorption needs to be investigated.

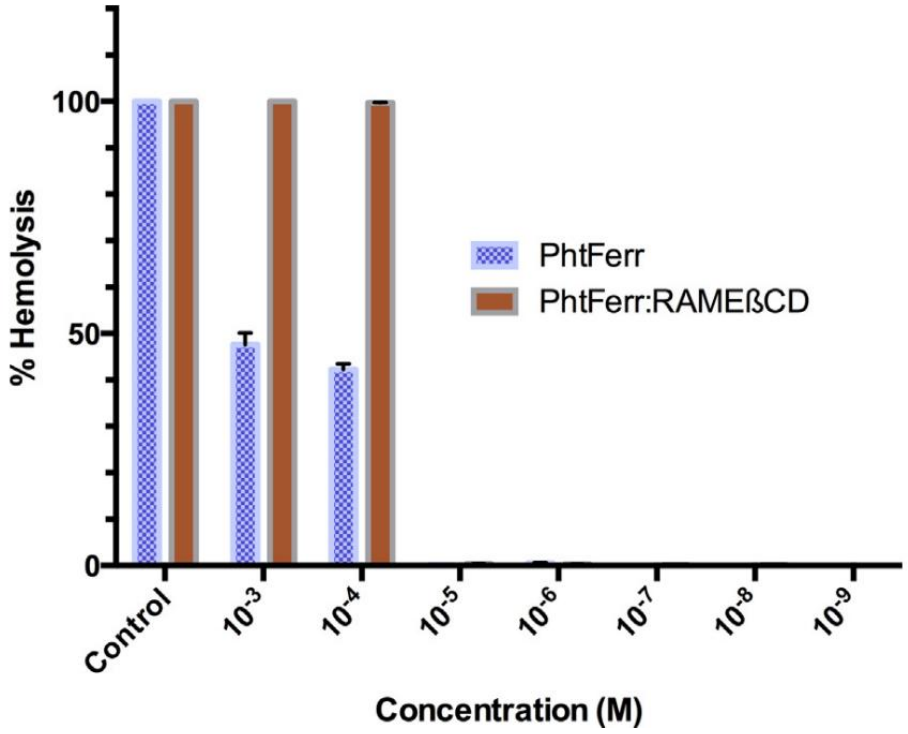

Fig. 11. Hemolysis properties of PhtFerr and PhtFerr:RAMEßCD after 1 h incubation-doses ranging from 10^{-3}M to 10^{-9}M. Data are expressed in percentage of hemolysis compared to the positive control (100%). Triton X-100 (1%) was used as positive control.

Conclusion

PhtFerr is very lipophilic and has a complex structure that, at first glance, could be complexed by 4 CDs. This kind of complex has rarely been completely studied, as many interactions can occur leading to a complex interpretation. The complete insolubility in water (i.e., below detectable concentration with usually analytical methods) increases the difficulty of its characterization.

The first experiment usually done to test the solubilization properties of CDs is the phase-solubility study initially described by Higuchi and Connors in 1965 (Higuchi and Connors, 1965). The best effect was obtained with methylated CDs and confirmed the results obtained by Buriez et al. (Buriez et al., 2008), who have demonstrated that the complexation of the ferrocene moiety is due to its very high lipophilicity.

It is also well known that methylated CDs have good solubilization properties. This solubility increases as the number of methyl groups reaches approximately 13-14 and then decreases as the number of substituents approaches 21 (Szente and Szejtli, 1999).

The phase-solubility experiment also demonstrated that the complexation does not have a 1:1 stoichiometry. This was not surprising because at least 3 other moieties could interact with the PhtFerr, but this possibility has not been previously demonstrated.

Molecular modeling can provide accurate information about the inclusion process (Stefano Alcaro and Ortuso, 2004). The inclusion of all moieties at the same time (i.e., ferrocene, phthalimidylpropyl, 2 phenols) is not possible due to the steric hindrance of the 1:4 system. The 1:3 systems are possible but do not seem very relevant; the hindrance leads to less deep inclusion into the CD cavity. However, various 1:2 and 1:1 complexes seem mostly present in aqueous solutions.

Some experiments have confirmed our hypothesis. First, an interaction of the phenol, phthalimidylpropyl and ferrocenyl groups have been observed in our NMR experiment. Second, the inclusion of the phthalimidylpropyl was detected using UV-vis spectrophotometry with an apparent 1:1 interaction observed by the Benesi-Hildebrand method.

The final PhtFerr:RAMEßCD was freeze-dried and tested for its pharmaceutical properties. The complex is readily soluble in water and keeps its pharmacological activity against U87 tumor cells (IC_{50} = 0.028 ± 0.007 µM *vs.* 0.018 ± 0.003 µM for PhtFerr). Nevertheless, the intravenous administration of this kind of complex can be limited by the hemolytic properties of methylated cyclodextrins. Hence, hemolysis was assessed and observed above 10^{-4} M. Due to the strong efficiency of PhtFerr, we think that it is possible to maintain the concentration of CD below 10^{-5} M. Blood brain barrier transport (BBB) is another hurdle. It is well known that pure CDs cannot cross the blood brain barrier. In the case of complexes, CDs increase the permeability by increasing the drug solubility (Vyas and Saraf, 2008), making the drug available at the surface of the of biological barrier. Even after the necessary

dissociation, the molecular mass of PhtFerr (583 Da) can limit the BBB transport: the concept of molecular mass threshold (400 – 600 Da) limiting BBB transport was advanced by Levin et al. (1980); nevertheless, there are occasional exceptions such as 2',7'-bis(2-carboxyethyl)-5(6)-carboxyfluorescein tetraacetoxymethyl ester (BCECF-AM), which has a molecular mass of 809 Da (Hirohashi et al., 1997; Pardridge, 1998) and crosses the BBB.

This complex must be tested in further experiments on a murine glioma model.

Acknowledgements

The authors wish to thank Michel Huché for molecular modeling advice and Mohamed Othman for extensive discussions. We thank the Agence Nationale de la Recherche for the financial support (ANR 2010 BLAN 7061 blanc Mecaferrol).

Fenten Najlaoui received a scholarship from the University of Carthage (Tunisia).

References

Alfonsi, R., Attivi, D., Astier, A., Socha, M., Morice, S., Gibaud, S., 2013. Characterization of mitotane (o,p′-DDD) – cyclodextrin inclusion complexes: phase-solubility method and NMR. Ann Pharm Fr 71, 186-192.

Allard, E., Huynh, N.T., Vessieres, A., Pigeon, P., Jaouen, G., Benoit, J.P., Passirani, C., 2009. Dose effect activity of ferrocifen-loaded lipid nanocapsules on a 9L-glioma model. Int J Pharm 379, 317-323.

Allard, E., Passirani, C., Garcion, E., Pigeon, P., Vessières, A., Jaouen, G., Benoit, J.-P., 2008. Lipid nanocapsules loaded with an organometallic tamoxifen derivative as a novel drug-carrier system for experimental malignant gliomas. J Controlled Release 130, 146-153.

Alvarez-Nunez, F.A., Yalkowsky, S.H., 1999. Buffer capacity and precipitation control of pH solubilized phenytoin formulations. Int J Pharm 185, 45-49.

Banchero, M., Ronchetti, S., Manna, L., 2013. Characterization of ketoprofen/methyl-β-cyclodextrin complexes prepared using supercritical carbon dioxide. J Chem.

Becherirat, S., Lanhers, M.-C., Socha, M., Yemloul, M., Astier, A., Loboda, C., Aniceto, N., Gibaud, S., 2013. The antitumor effects of an arsthinol–cyclodextrin complex in a heterotopic mouse model of glioma. Eur J Pharm Biopharm 85, 560-568.

Ben Zirar, S., Astier, A., Muchow, M., Gibaud, S., 2008. Comparison of nanosuspensions and hydroxypropyl-beta-cyclodextrin complex of melarsoprol: pharmacokinetics and tissue distribution in mice. Eur J Pharm Biopharm 70, 649-656.

Benesi, H.A., Hildebrand, J.H., 1949. A Spectrophotometric Investigation of the Interaction of Iodine with Aromatic Hydrocarbons. J Am Chem Soc 71, 2703-2707.

Biot, C., François, N., Maciejewski, L., Brocard, J., Poulain, D., 2000. Synthesis and antifungal activity of a ferrocene–fluconazole analogue. Bioorganic Med Chem Lett 10, 839-841.

Biot, C., Glorian, G., Maciejewski, L.A., Brocard, J.S., Domarle, O., Blampain, G., Millet, P., Georges, A.J., Abessolo, H., Dive, D., Lebibi, J., 1997. Synthesis and Antimalarial Activity in Vitro and in Vivo of a New Ferrocene−Chloroquine Analogue. J Med Chem 40, 3715-3718.

Bittner, B., Mountfield, R., 2002. Intravenous administration of poorly soluble new drug entities in early drug discovery: the potential impact of formulation on pharmacokinetic parameters. Curr Opin Drug Discov 5, 59-71.

Buriez, O., Heldt, J.M., Labbé, E., Vessières, A., Jaouen, G., Amatore, C., 2008. Reactivity and Antiproliferative Activity of Ferrocenyl–Tamoxifen Adducts with Cyclodextrins against Hormone-Independent Breast-Cancer Cell Lines. Chemistry 14, 8195-8203.

Çelik, S.E., Özyürek, M., Tufan, A.N., Güçlü, K., Apak, R., 2011. Spectroscopic study and antioxidant properties of the inclusion complexes of rosmarinic acid with natural and derivative cyclodextrins. Spectrochim Acta Mol Biomol Spectrosc 78, 1615-1624.

Chalumot, G., Yao, C., Pino, V., Anderson, J.L., 2009. Determining the stoichiometry and binding constants of inclusion complexes formed between aromatic compounds and beta-cyclodextrin by solid-phase microextraction coupled to high-performance liquid chromatography. J Chromatogr A 1216, 5242-5248.

Chatjigakis, A.K., Donze, C., Coleman, A.W., Cardot, P., 1992. Solubility behavior of .beta.-cyclodextrin in water/cosolvent mixtures. Anal Chem 64, 1632-1634.

Chelli, S., Majdoub, M., Jouini, M., Aeiyach, S., Maurel, F., Chane Ching, K.I., Lacaze, P.C., 2007. Host–guest complexes of phenol derivatives with β-cyclodextrin: an experimental and theoretical investigation. J Phys Org Chem 20, 30-43.

Citta, A., Folda, A., Bindoli, A., Pigeon, P., Top, S., Vessieres, A., Salmain, M., Jaouen, G., Rigobello, M.P., 2014. Evidence for targeting thioredoxin reductases with ferrocenyl quinone methides. A possible molecular basis for the antiproliferative effect of hydroxyferrocifens on cancer cells. J Med Chem 57, 8849-8859.

Craig Jordan, V., 1992. The role of tamoxifen in the treatment and prevention of breast cancer. Curr Probl Cancer 16, 134-176.

Dotsikas, Y., Kontopanou, E., Allagiannis, C., Loukas, Y.L., 2000. Interaction of 6-p-toluidinylnaphthalene-2-sulphonate with β-cyclodextrin. J Pharm Biomed Anal 23, 997-1003.

El-Maradny, H.A., Mortada, S.A., Kamel, O.A., Hikal, A.H., 2008. Characterization of ternary complexes of meloxicam-HPbetaCD and PVP or L-arginine prepared by the spray-drying technique. Acta Pharm 58, 455-466.

Elečko, P., Foltínová, P., Sališová, M., Solčániová, E., Toma, Š., 1974. Synthesis, proton magnetic resonance spectra, and biological activity of haloacylferrocenes. Chemicke Zvesti 28, 94-99.

Fouda, M.F.R., Abd-Elzaher, M.M., Abdelsamaia, R.A., Labib, A.A., 2007. On the medicinal chemistry of ferrocene. Appl Organomet Chem 21, 613-625.

Gadomski, A., Ausloos, M., 2006. Agglomeration/Aggregation and Chaotic Behaviour in d-Dimensional Spatio-Temporal Matter Rearrangements Number-Theoretic Aspects. Springer-Verlag, Berlin/Heidelberg, pp. 275-294.

Gadomski, A., Kruszewska, N., Ausloos, M., Tadych, J., 2007. On the Harmonic-Mean Property of Model Dispersive Systems Emerging Under Mononuclear, Mixed and Polynuclear Path Conditions, in: Schadschneider, A., Pöschel, T., Kühne, R., Schreckenberg, M., Wolf, D.E. (Eds.), Traffic and Granular Flow'05. Springer, Berlin, Heidelberg, pp. 283-296.

Gadomski, A., Rubí, J.M., Łuczka, J., Ausloos, M., 2005. On temperature- and space-dimension dependent matter agglomerations in a mature growing stage. Chem Phys 310, 153-161.

Gibaud, S., Attivi, D., 2012. Microemulsions for oral administration and their therapeutic applications. Exp Opin Drug Deliv 9, 937-951.

Gibaud, S., Zirar, S.B., Mutzenhardt, P., Fries, I., Astier, A., 2005. Melarsoprol-cyclodextrins inclusion complexes. Int J Pharm 306, 107-121.

Hansen, M., Nielsen, S., 1989. Re-examination and further development of a precise and rapid dye method for measuring cell growth/cell kill. J Immunol Meth 119, 203-210.

Higuchi, T., Connors, K., 1965. Phase-solubility techniques. Adv Anal Chem Instrum 4, 117-212.

Hillard, E.A., Vessières, A., Jaouen, G., 2010. Ferrocene Functionalized Endocrine Modulators as Anticancer Agents. Top Organomet Chem 32, 81-117.

Hirohashi, T., Terasaki, T., Shigetoshi, M., Sugiyama, Y., 1997. In vivo and in vitro evidence for nonrestricted transport of 2',7'-bis(2-carboxyethyl)-5(6)-carboxyfluorescein tetraacetoxymethyl ester at the blood-brain barrier. J Pharmacol Exp Ther 280, 813-819.

Itoh, T., Shirakami, S., Ishida, N., Yamashita, Y., Yoshida, T., Kim, H.-S., Wataya, Y., 2000. Synthesis of novel ferrocenyl sugars and their antimalarial activities. Bioorg Med Chem Lett 10, 1657-1659.

Jaouen, G., Top, S., 2013. The Ferrocifen Family as Potent and Selective Antitumor Compounds: Mechanisms of Action, in: Pombeiro, A.J.L. (Ed.), Advances in Organometallic Chemistry and Catalysis. John Wiley & Sons, Inc., Hoboken, New Jersey, pp. 563-580.

Jodál, I., Nánási, P., Szejtli, J., 1988. Investigation of the Hemolytic Effect of the Cyclodextrin Derivatives, in: Huber, O., Szejtli, J. (Eds.), Advances in Inclusion Science Springer Netherlands, Dordrecht, pp. 421-425.

Kondapi, A.K., Satyanarayana, N., Saikrishna, A.D., 2006. A study of the Topoisomerase II activity in HIV-1 replication using the ferrocene derivatives as probes. Arch Biochem Biophys 450, 123-132.

Laine, A.L., Adriaenssens, E., Vessieres, A., Jaouen, G., Corbet, C., Desruelles, E., Pigeon, P., Toillon, R.A., Passirani, C., 2013. The in vivo performance of ferrocenyl tamoxifen lipid nanocapsules in xenografted triple negative breast cancer. Biomaterials 34, 6949-6956.

Levin, V.A., 1980. Relationship of octanol/water partition coefficient and molecular weight to rat brain capillary permeability. J Med Chem 23, 682-684.

Madan, J., Gundala, S.R., Baruah, B., Nagaraju, M., Yates, C., Turner, T., Rangari, V., Hamelberg, D., Reid, M.D., Aneja, R., 2014. Cyclodextrin Complexes of Reduced Bromonoscapine in Guar Gum Microspheres Enhance Colonic Drug Delivery. Mol Pharm 11, 4339-4349.

Malagoli, D., 2007. A full-length protocol to test hemolytic activity of palytoxin on human erythrocytes. ISJ - Invertebr Surviv J 4, 92-94.

Messina, P., Labbé, E., Buriez, O., Hillard, E.A., Vessières, A., Hamels, D., Top, S., Jaouen, G., Frapart, Y.M., Mansuy, D., Amatore, C., 2012. Deciphering the Activation Sequence of Ferrociphenol Anticancer Drug Candidates. Chemistry 18, 6581-6587.

Nguyen, A., Marsaud, V., Bouclier, C., Top, S., Vessieres, A., Pigeon, P., Gref, R., Legrand, P., Jaouen, G., Renoir, J.-M., 2008. Nanoparticles loaded with ferrocenyl tamoxifen derivatives for breast cancer treatment. Int J Pharm 347, 128-135.

Nguyen, A., Vessières, A., Hillard, E.A., Top, S., Pigeon, P., Jaouen, G., 2007. Ferrocifens and Ferrocifenols as New Potential Weapons against Breast Cancer. CHIMIA Int J Chem 61, 716-724.

Ornelas, C., 2011. Application of ferrocene and its derivatives in cancer research. New J Chem 35, 1973-1985.

Pardridge, W.M., 1998. CNS Drug Design Based on Principles of Blood-Brain Barrier Transport. J Neurochem 70, 1781-1792.

Petrovski, Ž., Norton de Matos, M.R.P., Braga, S.S., Pereira, C.C.L., Matos, M.L., Gonçalves, I.S., Pillinger, M., Alves, P.M., Romão, C.C., 2008. Synthesis, characterization and antitumor activity of 1,2-disubstituted ferrocenes and cyclodextrin inclusion complexes. J Organomet Chem 693, 675-684.

Pigeon, P., Gormen, M., Kowalski, K., Muller-Bunz, H., McGlinchey, M.J., Top, S., Jaouen, G., 2014. Atypical McMurry cross-coupling reactions leading to a new series of potent antiproliferative compounds bearing the key [ferrocenyl-ene-phenol] motif. Molecules 19, 10350-10369.

Plazuk, D., Vessieres, A., Hillard, E.A., Buriez, O., Labbe, E., Pigeon, P., Plamont, M.A., Amatore, C., Zakrzewski, J., Jaouen, G., 2009. A [3]ferrocenophane polyphenol showing a remarkable antiproliferative activity on breast and prostate cancer cell lines. J Med Chem 52, 4964-4967.

Richard, M.A., Hamels, D., Pigeon, P., Top, S., Dansette, P.M., Lee, H.Z., Vessieres, A., Mansuy, D., Jaouen, G., 2015. Oxidative metabolism of ferrocene analogues of tamoxifen: characterization and antiproliferative activities of the metabolites. ChemMedChem 10, 981-990.

Rodgers, J., Jones, A., Gibaud, S., Bradley, B., McCabe, C., Barrett, M.P., Gettinby, G., Kennedy, P.G.E., 2011. Melarsoprol Cyclodextrin Inclusion Complexes as Promising Oral Candidates for the Treatment of Human African Trypanosomiasis. PLoS Negl Trop Dis 5, e1308.

Roger, M., Clavreul, A., Huynh, N.T., Passirani, C., Schiller, P., Vessieres, A., Montero-Menei, C., Menei, P., 2012. Ferrociphenol lipid nanocapsule delivery by mesenchymal stromal cells in brain tumor therapy. Int J Pharm 423, 63-68.

Rosenblum, M., 1965. Chemistry of the iron-group metallocenes, Part I. Intersciences, New York.

Scott, D.R., Becker, R.S., 1961. Comprehensive Investigation of the Electronic Spectroscopy and Theoretical Treatments of Ferrocene and Nickelocene. J Chem Phys 35, 516-531.

Soares da Silva, L.F.J., do Carmo, F.A., de Almeida Borges, V.R., Monteiro, L.M., Rodrigues, C.R., Cabral, L.M., de Sousa, V.P., 2011. Preparation and evaluation of lidocaine hydrochloride in cyclodextrin inclusion complexes for development of stable gel in association with chlorhexidine gluconate for urogenital use. Int J Nanomed 6, 1143-1154.

Stefano Alcaro, D.B., Ortuso, F., 2004. Molecular modeling of β-cyclodextrin inclusion complexes with pharmaceutical compounds. ARKIVOC 2004, 107.

Stupp, R., Roila, F., Group, E.G.W., 2009. Malignant glioma: ESMO clinical recommendations for diagnosis, treatment and follow-up. Ann Oncol 20 Suppl 4, 126-128.

Swarts, J., Neuse, E., Lamprecht, G., 1994. Synthesis and characterization of water-soluble polyaspartamide-ferrocene conjugates for biomedical applications. J Inorg Organomet Polym 4, 143-153.

Szente, L., Szejtli, J., 1999. Highly soluble cyclodextrin derivatives: chemistry, properties, and trends in development. Adv Drug Deliv Rev 36, 17-28.

Tahri, Z., Lepski, R., Hsieh, K.Y., Bendeif, E.E., Pillet, S., Durand, P., Woike, T., Schaniel, D., 2012. Properties of metastable linkage NO isomers in Na-2[Fe(CN)(5)NO]center dot 2H(2)O incorporated in mesopores of silica xerogels. Phys Chem Chem Phys 14, 3775-3781.

Tamura, H., Miwa, M., 1997. DNA Cleaving Activity and Cytotoxic Activity of Ferricenium Cations. Chem Lett, 1177-1178.

Togni, A., Hayashi, T., 1994. Ferrocenes. Wiley-VCH, Weinheim.

Top, S., Tang, J., Vessieres, A., Carrez, D., Provot, C., Jaouen, G., 1996. Ferrocenyl hydroxytamoxifen: a prototype for a new range of oestradiol receptor site-directed cytotoxics. Chem Commun, 955-956.

Top, S., Vessières, A., Leclercq, G., Quivy, J., Tang, J., Vaissermann, J., Huché, M., Jaouen, G., 2003. Synthesis, Biochemical Properties and Molecular Modelling Studies of Organometallic Specific Estrogen Receptor Modulators (SERMs), the Ferrocifens and Hydroxyferrocifens: Evidence for an Antiproliferative Effect of Hydroxyferrocifens on both Hormone-Dependent and Hormone-Independent Breast Cancer Cell Lines. Chemistry 9, 5223-5236.

Trapani, G., Latrofa, A., Franco, M., Pantaleo, M.R., Sanna, E., Massa, F., Tuveri, F., Liso, G., 2000. Complexation of zolpidem with 2-hydroxypropyl-beta-, methyl-beta-, and 2-hydroxypropyl-gamma-cyclodextrin: effect on aqueous solubility, dissolution rate, and ataxic activity in rat. J Pharm Sci 89, 1443-1451.

Vessieres, A., Top, S., Pigeon, P., Hillard, E., Boubeker, L., Spera, D., Jaouen, G., 2005. Modification of the estrogenic properties of diphenols by the incorporation of ferrocene. Generation of antiproliferative effects in vitro. J Med Chem 48, 3937-3940.

Vyas, A., Saraf, S., 2008. Cyclodextrin based novel drug delivery systems. J Incl Phenom Macrocycl Chem 62, 23-42.

Wang, Y., Pigeon, P., Top, S., Mc Glinchey, M.J., Jaouen, G., in press. A new generation of organometallic antitumor compounds: ferrocifens as precursors to novel quinone methides. Angew Chem DOI: 10.1002/anie.201503048.

Wei, H., Quan, C.-Y., Chang, C., Zhang, X.-Z., Zhuo, R.-X., 2010. Preparation of Novel Ferrocene-Based Shell Cross-Linked Thermoresponsive Hybrid Micelles with Antitumor Efficacy. J Phys Chem 114, 5309-5314.

Xiong, Q., Zhang, M., Zhang, Z., Shen, W., Liu, L., Zhang, Q., 2014. Anti-tumor drug delivery system based on cyclodextrin-containing pH-responsive star polymer: In vitro and in vivo evaluation. Int J Pharm 474, 232-240.

Yoe, J.H., Jones, A.L., 1944. Colorimetric Determination of Iron with Disodium-1,2-dihydroxybenzene-3,5-disulfonate. Ind Eng Chem Anal Ed 16, 111-115.

Zhang, J., 2008. Preparation, characterization, crystal structure and bioactivity determination of ferrocenyl–thiazoleacylhydrazones. Appl Organomet Chem 22, 6-11.

Supporting information

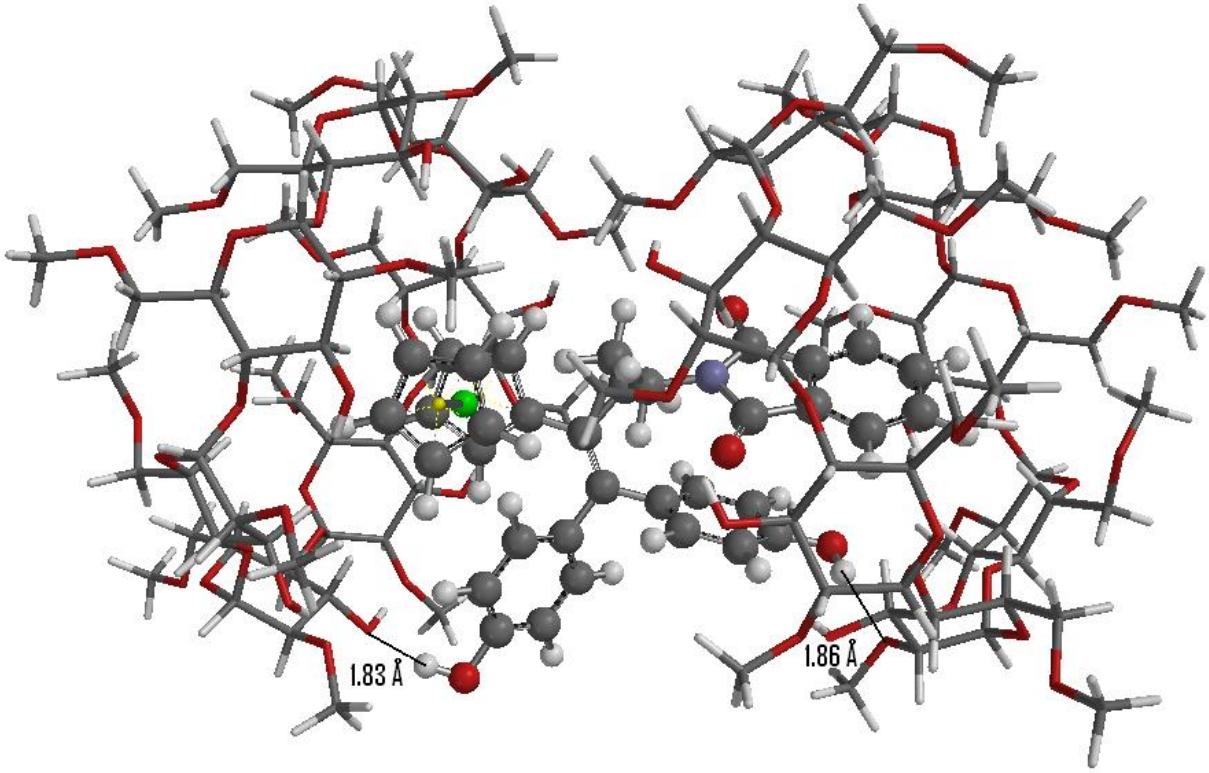

Supplementary Fig. 1. Inclusion of ferrocenyl and phthalimidyl groups with two CD (DMβCD, wide side), with indication of the hydrogen bonds between the phenol groups and the CD.

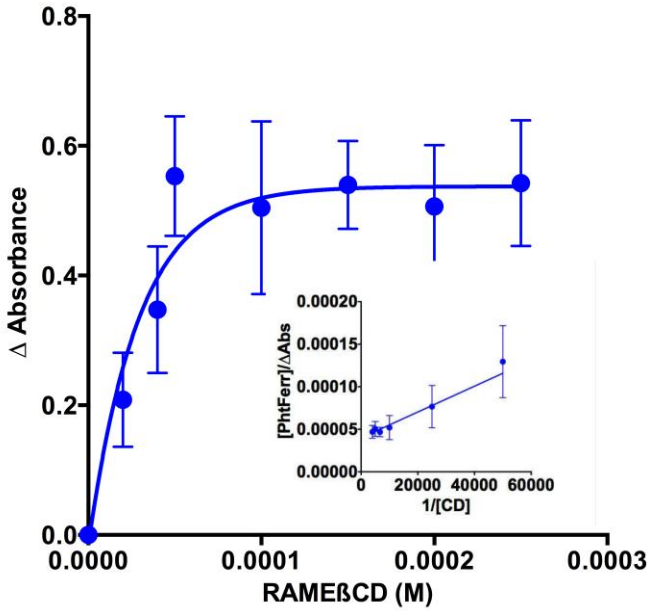

Supplementary Fig. 2. Mole–ratio titration plots of PhtFerr (2.5×10^{-5} M in 1% (v/v) DMSO/water) by RAMEβCD. The formation of the complex was monitored at 310 nm. Inset: Double reciprocal plots (Benesi-Hildebrand plots).

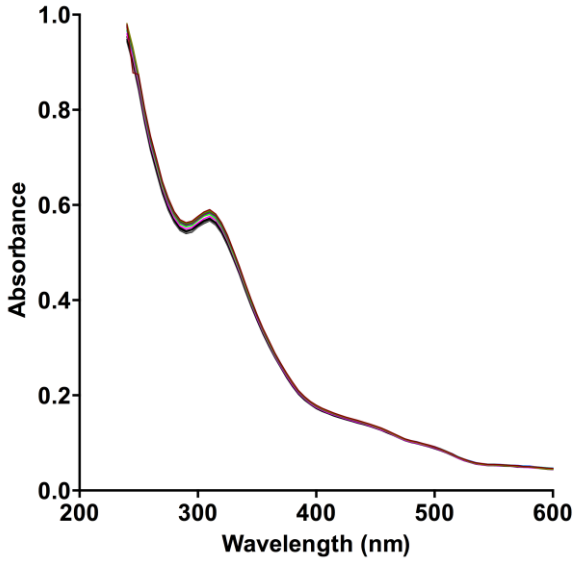

Supplementary Fig. 3. Spectra of PhtFerr ($2.5. 10^{-5}$ M). The first spectrum was obtained in water with 1%DMSO. The addition of various amount of HPβCD produced a hyperchromic effect especially at 310 nm.